ARMY RESEARCH LABORATORY

Development of a Surrogate STANAG 4240 Fire Exposure

by Pauline M. Smith, William H. Ruppert, Christopher L. Mealy, Joshua B. Dinaburg, Jason E. Floyd, Daniel P. Verdonik, Patrick Taylor, and Noah Lieb

ARL-TR-6004 **May 2012**

NOTICES

Disclaimers

The findings in this report are not to be construed as an official Department of the Army position unless so designated by other authorized documents.

Citation of manufacturer's or trade names does not constitute an official endorsement or approval of the use thereof.

Destroy this report when it is no longer needed. Do not return it to the originator.

Army Research Laboratory
Aberdeen Proving Ground, MD 21005-5069

ARL-TR-6004 **May 2012**

Development of a Surrogate STANAG 4240 Fire Exposure

Pauline M. Smith and William H. Ruppert
Weapons and Materials Research Directorate, ARL

Christopher L. Mealy, Joshua B. Dinaburg, Jason E. Floyd,
Daniel P. Verdonik, Patrick Taylor, and Noah Lieb
Hughes Associates, Inc.

REPORT DOCUMENTATION PAGE	Form Approved OMB No. 0704-0188

1. REPORT DATE *(DD-MM-YYYY)*	2. REPORT TYPE	3. DATES COVERED (From - To)
May 2012	Final	11 February 2010

4. TITLE AND SUBTITLE
Development of A Surrogate STANAG 4240 Fire Exposure

5a. CONTRACT NUMBER

5b. GRANT NUMBER

5c. PROGRAM ELEMENT NUMBER

6. AUTHOR(S)
Pauline M. Smith, William H. Ruppert, Christopher L. Mealy,[*] Joshua B. Dinaburg,[*] Jason E. Floyd,[*] Daniel P. Verdonik,[*] Patrick Taylor,[*] and Noah Lieb[*]

5d. PROJECT NUMBER
AH84

5e. TASK NUMBER

5f. WORK UNIT NUMBER

7. PERFORMING ORGANIZATION NAME(S) AND ADDRESS(ES)
U.S. Army Research Laboratory
ATTN: RDRL-WMM
Aberdeen Proving Ground, MD 21005-5069

8. PERFORMING ORGANIZATION REPORT NUMBER
ARL-TR-6004

9. SPONSORING/MONITORING AGENCY NAME(S) AND ADDRESS(ES)

10. SPONSOR/MONITOR'S ACRONYM(S)

11. SPONSOR/MONITOR'S REPORT NUMBER(S)

12. DISTRIBUTION/AVAILABILITY STATEMENT
Approved for public release; distribution is unlimited.

13. SUPPLEMENTARY NOTES
[*]Hughes Associates, Inc., 3610 Commerce Dr., Ste. 817, Baltimore, MD 21227-1652

14. ABSTRACT
All ordnance systems must be classified for hazards that are often coupled with insensitive munitions in order to lower development costs and ensure that the ordnance performs as intended, but are less prone to violent reaction when subjected to external hazards. Traditionally, large-scale liquid hydrocarbon pool fire, often referred to as the fast-cook-off test, raises the ordnance temperature very quickly and evaluates how it reacts when engulfed in fire. Currently, the liquid fuel external fire is used to determine the type of reaction and time to reaction of the ordnance when exposed to a thermal insult. The test requires the complete ordnance package be completely engulfed within a liquid pool fire. The allowable hydrocarbons fuels have relatively high soot yields and therefore generate highly-radioactive thermal environments to objects immersed within the fire plume. There has been an international push to develop alternative fuel fire exposures due to lack of control over the current fire scenario and the environmental implications associated with the hydrocarbon pool fire. The alternative methods are more environmentally sustainable than the baseline test method, produce less soot, do not use HAPs, and pose a lower risk for occupational and environmental exposures. This report summarizes alternative fuel fire exposures and additional benefits over the existing liquid fuel fire exposure. The benefits considered in this work were with respect to cost of operation, added control over exposure, and environmental impact.

15. SUBJECT TERMS
surrogate, STANAG, fire exposure, fuel fire, heat flux

16. SECURITY CLASSIFICATION OF:			17. LIMITATION OF ABSTRACT	18. NUMBER OF PAGES	19a. NAME OF RESPONSIBLE PERSON
a. REPORT	b. ABSTRACT	c. THIS PAGE			Pauline Smith
Unclassified	Unclassified	Unclassified	UU	94	19b. TELEPHONE NUMBER (*Include area code*) 410-306-0899

Contents

List of Figures

List of Tables

1. Introduction

In the United States, all ordnance systems must be hazard classified (*1*). In the late 1980s, this hazard classification was coupled with insensitive munitions (IM) testing in order to lower development costs as well as ensure that the ordnance performs as intended but are less prone to violent reaction when subjected to external hazards (i.e., impact, shock, and fire). As a result of recent events involving the destruction of ordnance depots, there has been a strong trend towards classifying all new munitions and weapons systems as IM. An IM is defined as a munition that will reliably fulfill performance, readiness and operational requirements on demand, but will minimize the violence of a reaction and subsequent collateral damage when subjected to unplanned stimuli or threat. Traditionally, the hazard/IM classification process for ordnance requires that a battery of tests be performed (*2*), one of which is a large-scale liquid hydrocarbon pool fire. This exposure, often referred to as the fast-cook-off (FCO) test, raises the ordnance temperature very quickly and evaluates how it reacts when it is engulfed in fire. Although required by MIL-STD-2105C (*2*), the test procedure for the liquid fuel fire test is specified in the NATO standard STANAG 4240 (*3*), and the passing criteria are identified in STANAG 4439 (*4*).

Currently, as described in STANAG 4240 (*3*), the liquid fuel external fire is used to determine the type of reaction and time to reaction of the ordnance when exposed to a thermal insult. The test requires the complete ordnance package, with packaging where appropriate, be completely engulfed within a liquid pool fire. The allowable hydrocarbons fuels are JP-4, JP-5, Jet A-1, AVCAT (NATO F-34/F-44), or commercial kerosene (Class C2/NATO F-58). These fuels have relatively high soot yields and therefore generate highly radiative thermal environments to objects immersed within the fire plume. The liquid pool fire must have dimensions 1 m (3.3 ft) larger than the ordnance on all sides and have sufficient fuel to run for 150% of the expected time to reaction. This estimated time to reaction is generally determined based upon empirical data obtained from small-scale testing and thermal property analysis. The large-scale pool fire is intended to produce a fuel-rich fire plume, thus ensuring that the heat transfer to the ordnance is primarily radiative. Thermal conditions proximate to the test article are monitored using a minimum of four thermocouples placed 40–60 mm (1.6–2.4 in) from the surface of the test article at positions fore, aft, port, and starboard along a horizontal plane through its center line. In order to be considered valid, average temperatures measured at these thermocouples must be greater than or equal to 800 °C (1472 °F). The time to reaction is measured from the time any two of these thermocouples reach 550 °C (1022 °F) until the time of reaction. The performance criteria identified for this test is that a reaction not more severe than burning (Type V) occur during the exposure.

An alternative fire test is also outlined in STANAG 4240. The "mini fuel fire" (MFF) can be used in situations where pollution is a concern or where the munition is not expected to have a type I, II, or III reaction. The munition must also have its largest dimension <0.63 m (2 ft) and weigh less than 50 kg (110 lb). The MFF still requires the full-scale munition to be tested but reduces the pool fire size to a 2-m (6.6-ft) square, with some added modifications.

As previously described, the execution of the STANAG 4240 FCO test protocol requires that a large quantity of liquid fuel be obtained, dispersed over a large area, and combusted for each ordnance tested. In general, this process poses substantial logistic, repeatability, and environmental problems. Logistical problems associated with the use of a liquid hydrocarbon fuel include obtaining and distributing the fuel in a safe manner and reasonable time frame while limiting the exposure of the fuel to the environment. Fuel cost must also be considered given that quite often, the quantity of fuel required to produce an acceptable exposure fire for large ordnance packages is very large.

The assurance of repeatability between FCO tests is very limited due to a variety of factors including variations in fuel composition, lack of control of fire exposure, and susceptibility of the fire plume to ambient wind conditions. Currently, establishing repeatability between two tests is very challenging given that the fuels specified in STANAG 4240 are all multi-constituent fuel blends. As a result, the fuels used can vary from manufacturer to manufacturer as well as based upon the season during which the test was conducted. This variance in fuel composition can impact the development and possibly the severity of the thermal environment created during a test. Another factor affecting the ability to conduct repeatable tests is the overall lack of control that is afforded to the test operator when conducting a large, liquid fuel pool fire. As stated earlier, the quantity of fuel used in a test is designed to be 50% more than that expected to cause a reaction; however, in the event a reaction does not occur, the test operator has no means of continuing the test. Thus, the test is wasted and the fire exposed ordnance now poses an extreme safety hazard. Finally, ambient wind conditions can have a significant impact on both the heat release rate and the thermal environment generated by the liquid fuel fire. While there is very little that can be done to control this impact, it is necessary to be aware of the potential for variation between tests due to wind.

The environmental problems associated with conducting the current STANAG 4240 fast cook-off test include both land based and airborne contamination due to contact with the unburned fuel and the production or large volumes of soot/combustion gases, respectively. Prior to the start of the STANAG 4240 exposure fire, large quantities of fuel are dispersed over a large area of land. While best efforts may be made to only pour the fuel into the containment area, it is not unreasonable to assume that some fraction of the fuel escapes the containment area and is exposed the neighboring ground, which over time can result in contamination of the ground. Furthermore, once ignited, the hydrocarbon fuel is burning relatively inefficiently, thus producing large volumes of soot and combustion gases which contaminate the environment.

Recently, there has been an international push to develop/institute alternative fuel fire exposures to be used in place of the STANAG 4240 fire scenario due to an overall lack of control over the current fire scenario as well as the environmental implications associated with the hydrocarbon pool fire. A summary of the international interest and the steps that have been taken to date was outlined by Tanner (*5*). These steps include:

- Identifying a means by which an alternative fuel fire can be accepted under existing standards,
- Identifying the key aspects of the alternative fuel fire development that should be addressed, and
- Developing preliminary gaseous/alternative fuel fire exposures and performing comparative testing.

Also pointed out in this summary was the fact that STANAG 4240 does not permit the use of propane, nor any other non-liquid fuel, but STANAG 4439 and AOP-39 state that where environmental concerns dictate, alternate fuels such as propane or natural gas may be used if testing verifies that the overall test item heating rate, uniformity of spatial heating to the test item, and type of radiation heat transfer duplicate those produced by the hydrocarbon pool fire. Tanner (*5*) also indicates that an environmentally friendly alternative exposure is the goal and heat flux is the critical parameter dictating the acceptability of an alternative fuel fire exposure.

1.1 Scope

Based upon the overview provided by Tanner (*5*), a path forward was developed to address the items outlined. The first task undertaken was the development of a robust, fully-instrumented container that could be used to characterize the thermal response of an object to the various fire exposures. In order to be able to characterize the heat flux (i.e., critical parameter) imposed by various exposure fire scenarios, an instrumented package was specifically designed to measure the thermal exposure. The second task was to characterize the thermal exposure generated by the STANAG 4240 liquid fuel external fire exposure to serve as a baseline to which all alternative fuel fire exposures are compared. The third task was to address the fact that to date, a scientific basis for developing an alternative fuel (i.e., gaseous/liquid fuel spray) fire that produces an exposure equivalent to a liquid pool fire has not been established. Based upon this, two different alternative fuel exposure fire scenarios were developed to address the heating rate, spatial uniformity, and environmental issues put forth by Tanner (*5*). For this task, both liquid and gaseous fuel alternatives were developed such that if a non-liquid fuel is not accepted, a liquid fuel alternative with less environmental impact could be adopted. The final product of this work is a proof-of-concept on a reduced scale that the development of a gaseous equivalent is feasible and the identification of the benefits and potential issues related to the test method.

1.2 Objectives

The objectives of phases I and II of this task were to design, construct, characterize, and validate the suitability of an instrumented container that will be used in the characterization of both STANAG 4240 and alternative fuel fires. The objective of phase III of this test program was to characterize the thermal response of the instrumented container to the liquid fuel/external fire specified in STANAG 4240. This characterization included the standard flame temperature measurements prescribed by the test method as well as instrumented container surface temperatures and plate thermometer measurements. These data were compared to UL 1709 (*6*) furnace exposure data collected using the same instrumented container and will be used in future efforts to develop an equivalent gaseous fire test exposure.

The objective of the phase IV test program was to characterize the thermal response of the instrumented container to several alternative fuel fire exposures. The data collected in this testing will be compared to the data collected during phase III (standard STANAG 4240 test fires conducted using the same instrumented container). Thermal exposure comparisons will be made on the basis of average flame temperatures within the fire plume as well as both temperature and incident heat flux data collected at the surface of the instrumented container.

2. Phase I – Development of Instrumented Test Article

2.1 Test Article Development

The containers were designed and constructed to have the same external dimensions as the PA-124 military container. The PA-124 measures 28 × 14 × 48 cm (11.0 × 5.5 × 18.75 in) and is shown in figure 1.

Figure 1. PA-124 military container.

The instrumented containers were constructed from 6.3-mm (0.25-in)-thick carbon steel sheet and consisted of separate box and lid sections. The two pieces were constructed separately and assembled during instrumentation. They were assembled using eight threaded rods inserted through the walls of the lid and body of the container. This provided a tight seal while allowing the box to passively vent during the fire exposures, preventing a dangerous buildup of pressure within the box. A photograph of the instrumented container is provided in figure 2.

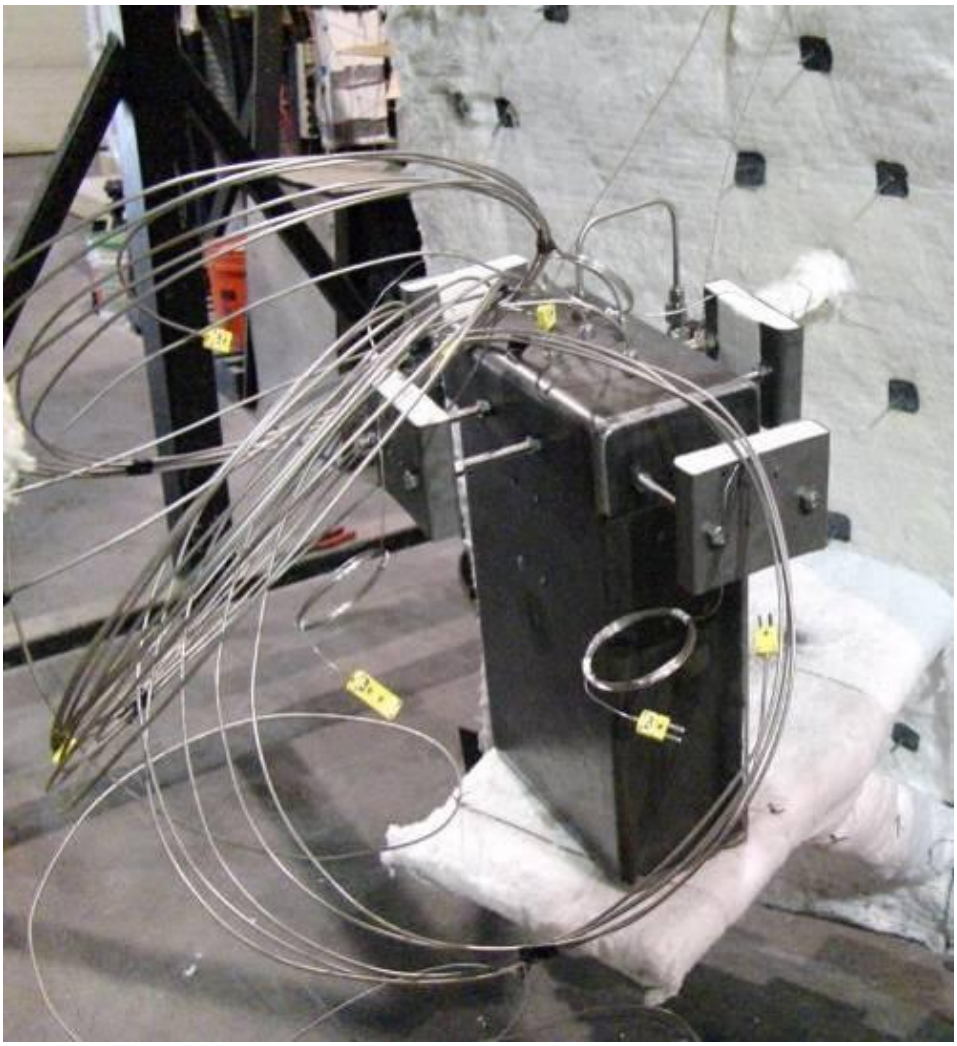

Figure 2. Photograph of one of the instrumented containers placed on furnace shelf.

The base of the container consists of five sealed sides with an open top. It measures 28 × 14 × 47 cm (11.0 × 5.5 × 18.5 in) externally. Each of the surfaces has a 3.2-mm (1/8-in) hole drilled in the center of the face. The holes were filled by welding to a depth of 3.2 mm (1/8 in) such that they allowed thermocouple insertion to one half the thickness of each internal wall of the container. The design drawings of the container base are shown in figures 3–5. Figure 3 is the top view, figure 4 is the front view, and figure 5 shows a close-up of a thermocouple hole in the container wall.

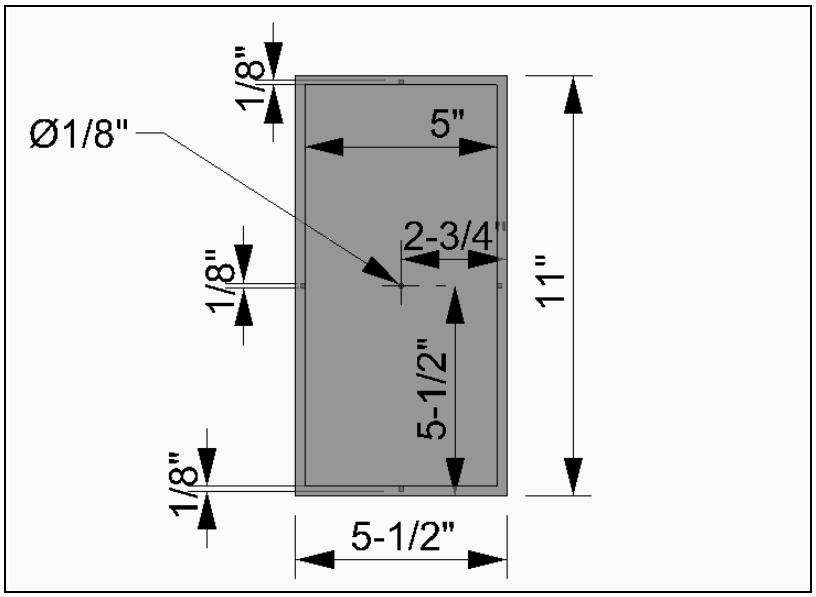

Figure 3. Top view of PA-124 surrogate container with 1/8-in diameter and depth holes highlighted.

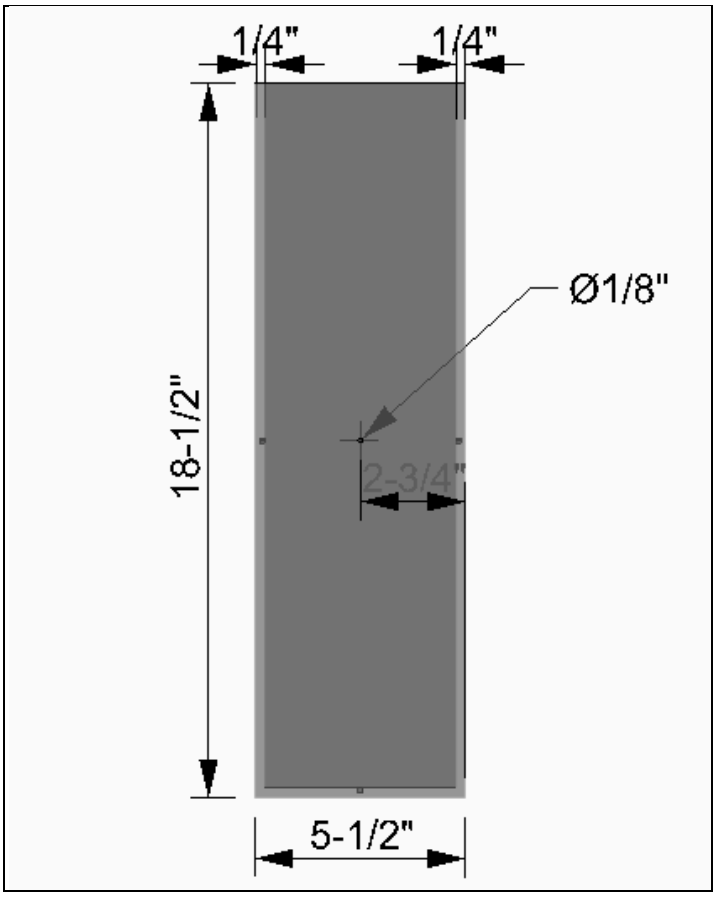

Figure 4. Front view of PA-124 surrogate container with internal wall thickness shown.

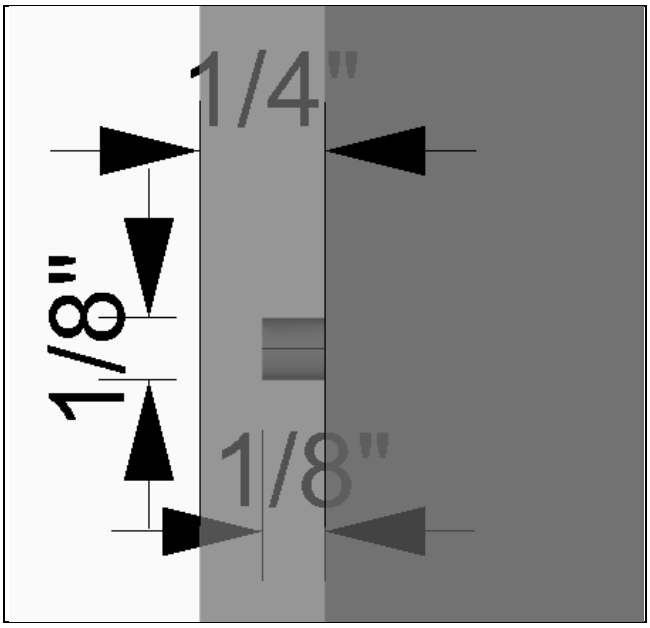

Figure 5. Cutaway view of thermocouple hole drilled into internal face of container.

A lid was constructed for the container to fit snugly over the top and allow insertion of instrumentation. The lid was also fabricated of 6.35-mm (0.25-in) carbon steel and had external dimensions of 29.2 × 15.2 × 7.6 cm (11.5 × 6 × 3 in), thus an internal space of 28 × 14 × 7 cm (11 × 5.5 × 2.75 in). There are five 8.3-mm (0.328-in) holes drilled in the top surface, with one in the exact center, two linear in the 15.2-cm (6-in) dimension centered 3.5 cm (1.325 in) from the center, and two linear in the 29.2-cm (11.5-in) dimension centered 7 cm (2.75 in) from the center. There is one 11.5-mm (0.453-in) hole drilled diagonal from center at 7 cm (2.75 in) and 3.5 cm (1.325 in) from the center aligned with the other holes. The design drawings of the container base lid are shown in figure 6.

The holes in the surface allowed for stainless steel bulkhead fittings to be inserted. Five SS-200-61 0.125-in bulkhead fittings were inserted into the five 0.328-in holes. These fittings allowed the 0.125-in-diameter thermocouples used to measure internal surface temperatures to be fixed in place once installed within the container.

Five thermocouples were mounted in place by bending the tips into the drilled holes and attaching to the side walls with one 1.25- × 5.0-cm (0.5- × 2-in) plate mounted 18.4 cm (7.25 in) from the top of the container. The TCs were also mounted with a 90° bracket 5.0-cm (2-in) wide, with two 1.25-cm (0.5-in) sides mounted 10 cm (4.0 in) below the top of the container. The plates compressed the thermocouples with 2.5 cm (1 in) number 6 pan-head machine screws and nuts. A photograph of the thermocouples mounted on the interior of the steel container is provided in figure 7, and a schematic outlining their installation is provided in figure 8. One SS-400-61 0.25-in stainless steel bulkhead fitting was provided as a pressure tap for making internal pressure measurements within the container during furnace exposures.

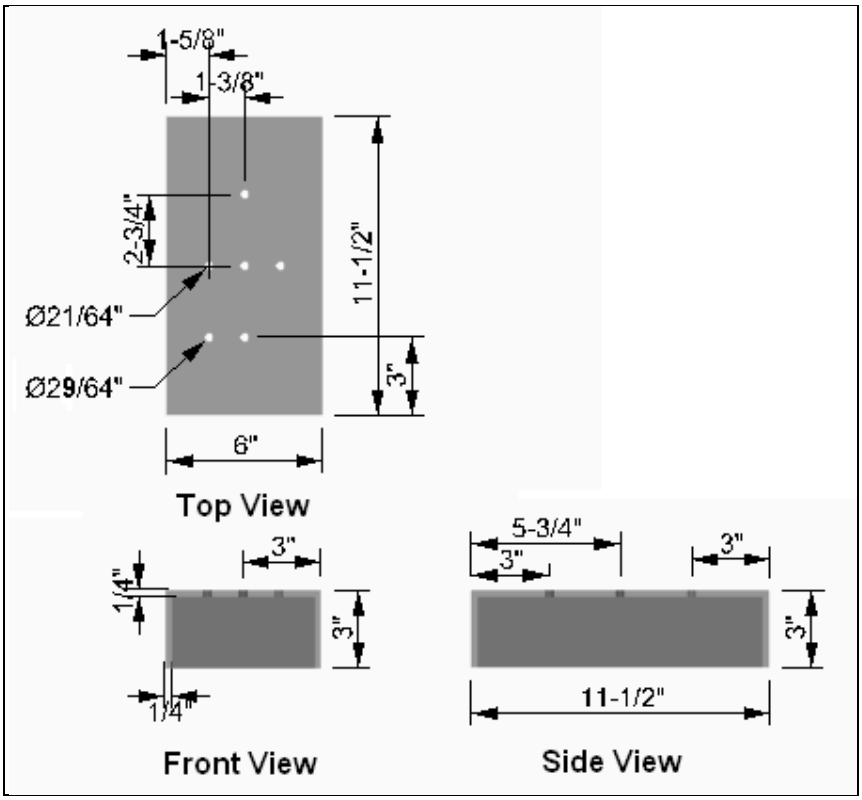

Figure 6. Dimensioned drawings of PA-124 instrumented container lid.

Figure 7. Photograph of thermocouples mounted on the interior surface of the containers as taken from the top looking into the container.

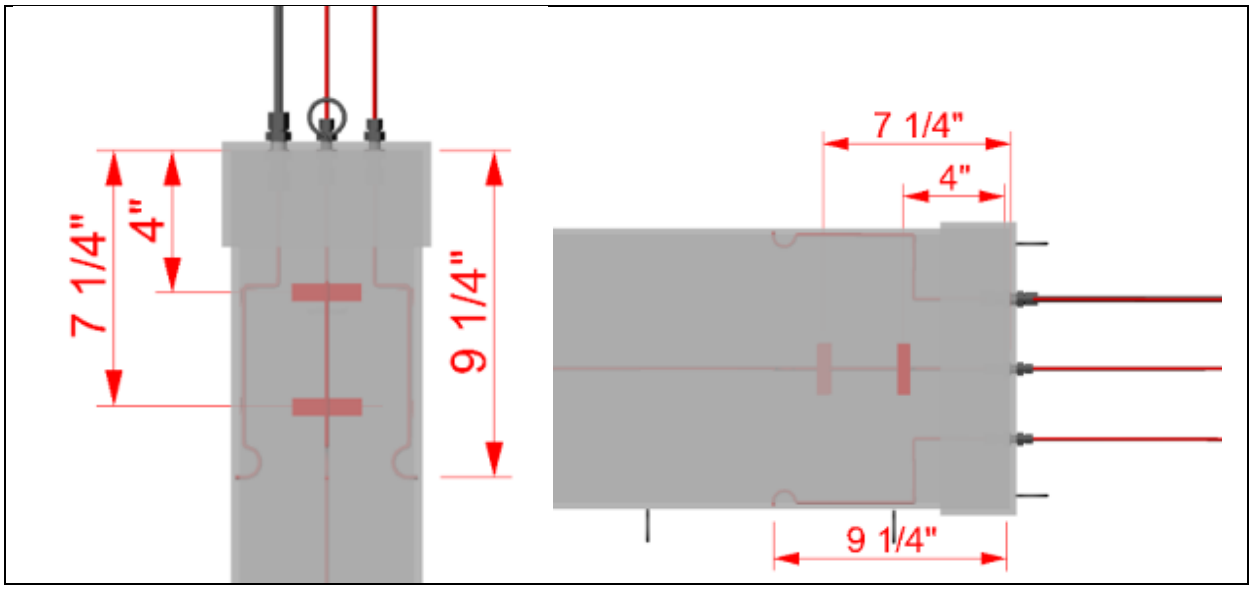

Figure 8. Thermocouple bending and mounting inside test container.

As shown in figure 2, the container was supported on a shelf welded to the furnace door. The shelf was placed at an elevation which, once the door was installed on the furnace, set the instrumented container in the geometric center of the furnace cavity. The shelf was wrapped in Fiberfrax insulation to prevent conduction losses from the test surrogate. This installation method will most likely result in the bottom of the container measuring lower temperatures than the other container sides. A schematic of the internal instrumentation installed on the containers, including mounting hooks, bulkhead fittings, thermocouples, and the pressure tap, is shown in figure 9.

Once all of the internal instrumentation was installed, the container was packed with ceramic fiber insulation (Unifrax Durablanket S with a nominal density of 96 kg/m^3 [6 lb/ft^3]) to reduce air volume and create adiabatic wall conditions. Furnace testing was used to determine if the fiber insulation could provide adequate and repeatable thermal resistance to the interior walls to validate that the walls replicate plate thermometers for characterizing heat flux.

In addition to the five wall-mounted thermocouples previously described, four plate thermometers (PTs) were installed around the perimeter of the containers to measure adiabatic surface temperatures. The plate thermometers were designed in general accordance with ISO 834 (*7*) and BS/EN 1363-1 (*8*), consisting of a sheet of 0.7-mm (0.024-in)-thick Inconel 601 100 × 225 mm (3.9 × 8.9 in). A 1-mm (0.040-in)-diameter, shielded and isolated Inconel thermocouple was pressed to the back of the sheet and secured in place by two strips of Inconel measuring 5.1 × 1.3 cm (2.0 × 0.5 in) screwed to the front plate. The plate assembly is shown in figure 10.

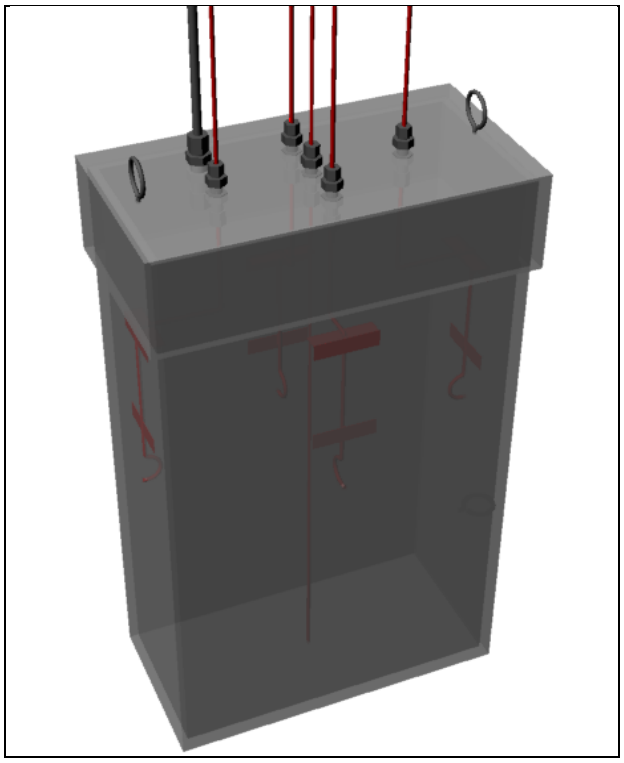

Figure 9. Schematic of PA-124 container surrogate with bulkhead fittings, internal thermocouples, pressure tap, and mounting hooks.

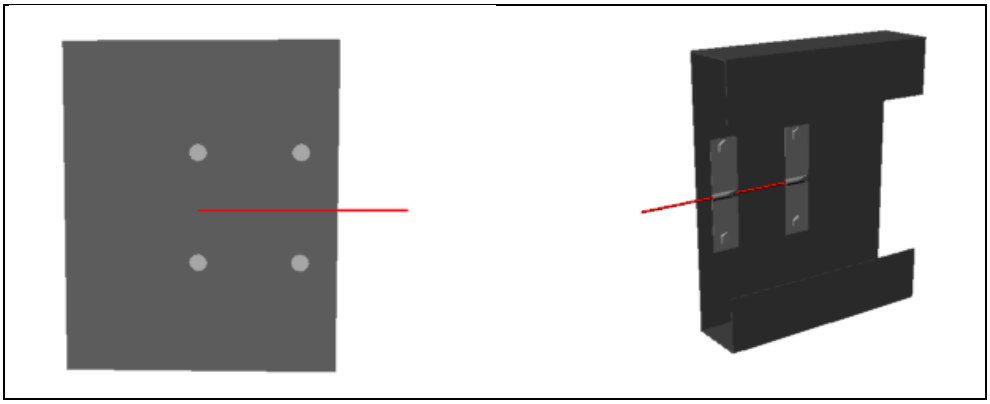

Figure 10. Plate thermometer assembly with TC attached by screwed on Inconel strips from front (left) and back (right).

The main Inconel sheet was folded around a piece of 2.5-cm (1-in)-thick Duraboard LD insulation such that the front surface measured 100 × 125 mm (3.9 × 4.9 in) and the insulation was compressed into the thermocouple and plate by the wrapped plate. The assembly with the insulation is shown in figure 11.

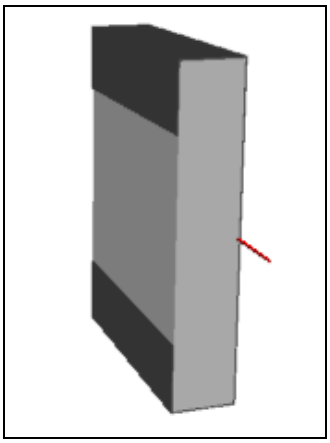

Figure 11. Plate Thermometer with insulation backing secured by bending main plate.

The PTs were placed around the four sides of the container and around the lid at a distance of 10 cm (4 in) from and oriented parallel to the surface. They were supported by two 9.5-mm (0.375-in) threaded rods running into the container lid and container and through the bent surfaces of the plate. They were not placed on the top or bottom container surfaces due to the small area of these faces. The PTs may act to shield the container from a small portion of the radiative flux from the pool fire. In order to reduce the impact of this on the wall-mounted thermocouples, the PTs were offset from the center of the container faces. In combination with the threaded rods, this should minimize the interference between the PTs and the wall thermocouples. An illustration of the vertically-oriented containers with PTs installed is provided in figure 12. The complete container assembly with all thermocouples, fittings, and PTs is shown in figure 13.

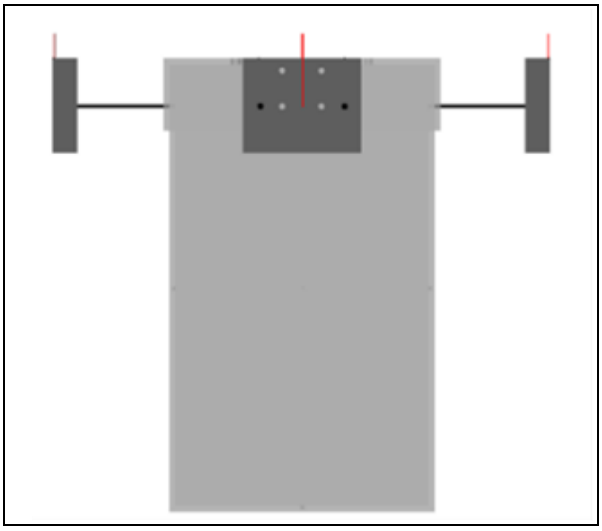

Figure 12. View of plate thermometer mounting assembly from side (left) and front (right).

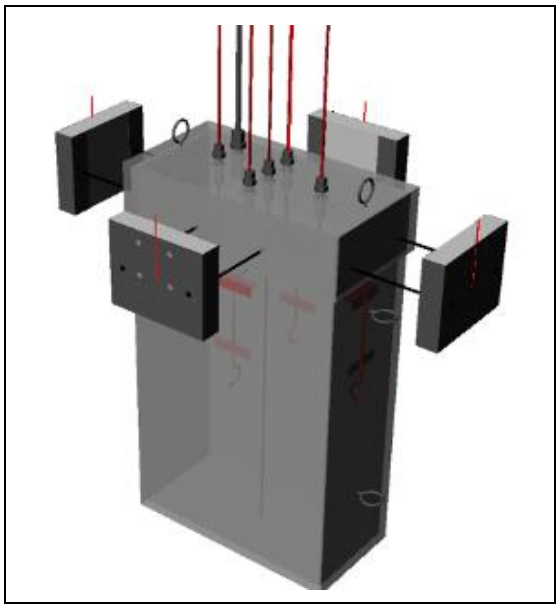

Figure 13. Completed instrumented container assembly with all fittings, thermocouples, and PTs.

2.2 Measurements and Analysis

Heat-flux estimates were made from the PT and wall temperatures. This procedure has been described by Ingason and Wickstrom (*9*). The temperatures of the steel were considered to approximate adiabatic surface temperatures due to the insulation material pressed to the unexposed sides.

The total heat flux, q_{tot}, is estimated as the sum of the incident radiated flux, q_{inc}, and the convective flux q_{conv}, minus the emitted radiated flux, q_{emi}. The total heat flux is shown in equation 1.

$$\dot{q}_{tot} = \dot{q}_{inc} - \dot{q}_{emi} + \dot{q}_{conv} \, . \tag{1}$$

Expanding the last two terms in equation 1 results in equation 2, where T_s is the surface temperature, h is the convective coefficient, T_∞ is the surrounding temperature, and ε is the surface emissivity:

$$\dot{q}_{tot} = \varepsilon(\dot{q}_{inc} - \sigma T_s^4) + h(T_\infty - T_s) \, . \tag{2}$$

The total heat flux can also be determined through heat balance as shown in equation 3, where q_{stor} is the heat retained in the surface to raise the temperature and q_{cond} is the heat conducted away from the surface through the insulation and surrounding metal plate or mounts.

$$\dot{q}_{tot} = \dot{q}_{stor} + \dot{q}_{cond} \, . \tag{3}$$

Expanding the right hand side of equation 3 yields equation 4, where ρ is the density of the steel, c is the specific heat capacity, δ is the plate thickness, ΔT is the change in temperature over the time interval Δt, and K_{cond} is the total thermal conductivity away from the plate.

$$\dot{q}_{tot} = \rho c \delta \frac{\Delta T_s}{\Delta t} + K_{cond}(T_s - T_\infty) \, . \tag{4}$$

Setting equation 2 equal to equation 4 and solving for the incident radiation heat flux yields equation 5:

$$\dot{q}_{inc} = \frac{\varepsilon \sigma T_s^4 + (h + K_{cond})(T_s - T_\infty) + \rho c \delta \frac{\Delta T_s}{\Delta t}}{\varepsilon} \, . \tag{5}$$

When the PT reaches a steady state condition or when the temperature is very high, the radiative component of the total heat flux will dominate over convection and conduction. During furnace testing, the calculated heat flux of the plates and box wall was compared to a total heat flux gauge installed in the furnace wall. This gauge provides a measure of both the incident radiative heat flux, estimated in equation 5, but also the convective heat transfer between the external gas and the gauge surface. The gauge surface is kept at a steady temperature using cooling water, thus the total convective flux is always significant. In order to account for the convective component of the heat flux gauge, the PT heat fluxes were modified by including the convective heat flux component expected between the hot gases and the gauge cooling water. The total heat flux to the PT and box wall surfaces will be calculated by equation 6 in units of W/m^2, where T_w is the estimated temperature of the cooling water, 30 °C (86 °F).

$$\dot{q}_{THF} = \frac{\varepsilon \sigma T_s^4 + (h + K_{cond})(T_s - T_\infty) + \rho c \delta \frac{\Delta T_s}{\Delta t}}{\varepsilon} + h(T_g - T_w) \, . \tag{6}$$

For these tests, the gas temperature, T_g, and the surrounding ambient temperature, T_∞, will be considered equal to the measured flame or furnace temperatures which is a valid assumption if the flame is considered to be optically thick. The calculation of total heat flux applied to the plate thermometers in equation 6 should accurately estimate the total heat flux that would be measured by a water-cooled heat flux gauge placed in the same location as the plate.

All terms in equation 6 are known or measured except for the plate emissivity, ε, and the heat transfer coefficients h and K_{cond}. The convective heat transfer coefficient has been assumed to equal 10 W/(m^2-K), as is recommended by Ingasson and Wickstrom (*9*). This value can be calculated by estimating the natural convection over a vertical plate by calculating the Rayleigh number at the film intermediate film temperature. The Rayleigh number is calculated as a function of gravity, g, the inverse of the film temperature, β, the difference between the surface and gas temperature, the size of the plate, L, the kinematic viscosity of the gas, ν, and the thermal diffusivity, α. The properties of the gas are all calculated at the film temperature and applied to equation 7.

$$Ra_L = \frac{g\beta(T_s - T_g)L^3}{\nu\alpha} \, . \tag{7}$$

Calculation of Rayleigh numbers for air over the range of temperatures expected for the furnace and pool exposure fires yields $Ra_L \approx 10^7$, which allows calculation of the Nusselt number for the plates to be calculated for laminar flow by equation 8 (*10*), where the Prandtl number, Pr, for air is estimated to be ~0.7 over the range of temperatures.

$$\overline{Nu}_L = 0.68 + \frac{0.670 Ra_L^{1/4}}{\left[1 + (0.492/Pr)^{9/16}\right]^{4/9}} \ . \tag{8}$$

Calculation of the range of Nusselt numbers expected yields ~$20 < \overline{Nu}_L < 30$. Finally, the convection coefficient, h, can be calculated by equation 9 for the size of the plate thermometer and the thermal conductivity of the air at the film temperature, k.

$$h = \frac{\overline{Nu}_L \cdot k}{L} \ . \tag{9}$$

Calculation confirms that in the range of temperatures expected for these experiments, a convective heat transfer coefficient of 10 W/m^2-K is considered appropriate to obtain fairly accurate estimates of the total heat flux. Similar calculations were performed for the horizontal plate conditions and yielded comparable results. For this experiment, the coefficient of 10 W/m^2-K will be applied to all plate orientations. In the temperature ranges expected for these fire tests, the radiation will dominate the heat transfer, and thus this approximation of the convection heat transfer coefficient should not significantly affect results.

The conductive heat-transfer coefficient was examined after heat flux correlations to measured results were performed. For these experiments, no additional K_{cond} was necessary to get agreement with the measured heat flux data. In this analysis, the sum of h and K_{cond} was estimated to be 10 W/m^2-K. Experimental analysis of the emissivity as a function of temperature was performed by placing a plate thermometer beneath a conical heater and observing the surface with an optical pyrometer. The emissivity setting of the pyrometer was adjusted such that the temperature reading would agree with the plate thermometer thermocouple over a range of expected temperatures. The emissivity as a function of temperature was calculated through equation 10:

$$\mathrm{T} < 548\mathrm{K} \Rightarrow \varepsilon = 1$$

$$548\ \mathrm{K} < \mathrm{T} < 623\ \mathrm{K} \Rightarrow \varepsilon = 0.97$$

$$623\ \mathrm{K} < \mathrm{T} \Rightarrow \varepsilon = -0.156 ln\left(\frac{9}{5}(T_s - 273) + 32\right) + 1.9736 \ . \tag{10}$$

The specific heat capacities of the steel and the Inconel plates have been determined over the range of expected test temperatures. Linear interpolation was used to calculate the heat capacity between each set of given values in table 1. The large spike in the carbon steel heat capacity at 768 °C (1414 °F) occurs due to a phase shift occurring at the Curie temperature of the material. This phase shift is represented numerically by a large, rapid spike in the specific heat capacity.

Table 1. Specific heat capacity of steel and inconel as a function of temperature (*11*).

Carbon Steel Box			600 Series Inconel		
Temperature		Specific Heat Capacity	Temperature		Specific Heat Capacity
(C°)	(F°)	(J/kg-K)	(C°)	(F°)	(J/kg-K)
0	32	439.53	0	32	439.53
75	167	502.32	300	572	544.18
200	392	565.11	>300	>572	544.18
400	752	627.9	—	—	—
600	1112	711.62	—	—	—
700	1292	837.2	—	—	—
763	1405	837.2	—	—	—
768	1414	6898.528	—	—	—
773	1423	703.248	—	—	—
950	1742	669.76	—	—	—
>950	>1742	669.76	—	—	—

The surface temperatures were measured at each location at a rate of 1 Hz, and T_∞ was assumed to be equal to the measured furnace temperature. The remaining storage terms for both the plate thermometers and the box wall surfaces are shown in table 2.

Table 2. Steel material properties for calculation of heat storage for plate thermometers and steel box surrogate.

Parameter			Inconel Plate Thermometers	Carbon Steel Box Wall
Symbol	Description	Units		
ρ	Density	[kg/m^3]	8110	7860
		[lb/in^3]	0.293	0.284
δ	Plate thickness	[mm]	0.7	6.36
		[in]	0.0276	0.25

Note that the steel box wall thickness used for calculations is the total thickness of the steel wall. The thermocouple is imbedded at a depth of one half the wall thickness, and thus the actual steel thickness external to the measurement is 3.18 mm (0.125 in). Calibration data taken with the box and heat flux gauges, however, show much better agreement to the measured heat flux during non-steady state exposures when the total wall thickness is used in equation 6. This is due to the heat storage occurring throughout the plate, and not only at the thermocouple location.

3. Phase II – Calibration of Instrumented Test Article

3.1 Intermediate-Scale Furnace Exposure

The intermediate-scale furnace used in this task consisted of a steel box insulated internally with ceramic fiber block insulation material. The inside opening of the furnace measured 91.4 × 91.4 × 121.9 cm (36 × 36 × 48 in), as shown in figure 14. As mentioned earlier, the

instrumented container was installed atop an insulated shelf and placed within the furnace. The shelf was constructed such that the once installed the instrumented container was located in the geometric center of the furnace cavity. The controlling components of the intermediate-scale furnace are shown in figure 15.

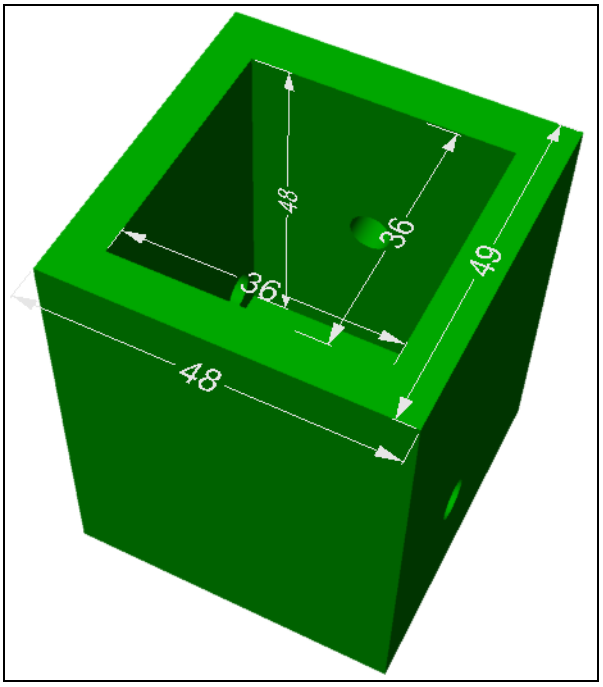

Figure 14. HAI laboratory furnace dimensions (inches).

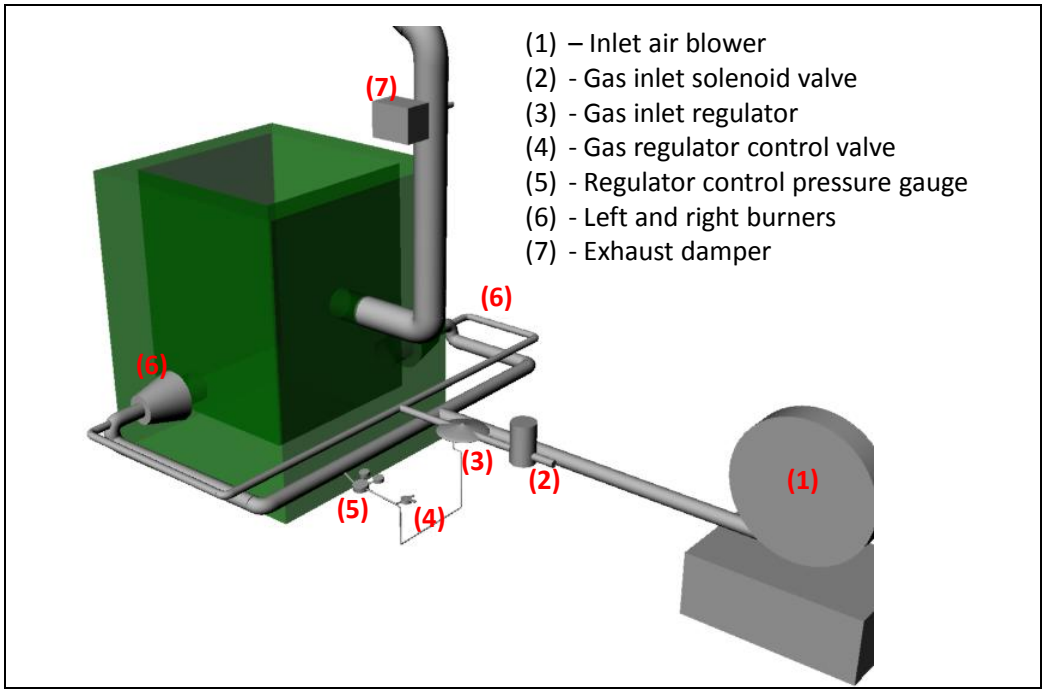

Figure 15. HAI laboratory furnace schematic with labeled parts list.

The furnace is driven by two burners entering from opposite sides, (6) in figure 15. The burners contain spark igniters and a mixing chamber with an air and a natural gas inlet. The internal temperature of the furnace can be regulated by controlling the air to fuel ratio in the mixing chambers. Air is blown into the system using a 4.7 m^3/s (10,000 cfm) blower fan (1) that feeds directly into the burners. Natural gas enters the system through a controlled solenoid valve (2) and an adjustable regulator (3). The regulator controls the flow rate of natural gas allowed to enter the system. The regulator is controlled by providing pressurized air to a control inlet. The pressurized air is provided by a connection to the air inlet line. The pressure of the air on the control is monitored using a gas regulator and pressure gauge (5) and a blow-off valve (4). The greater the pressure applied to the fuel regulator, the more natural gas is allowed to enter the mixing chambers in the burners. Continuous monitoring and control of the blow-off valve allowed the operator to maintain specific temperatures within the furnace. In addition, proper operating pressure (~–5 Pa) was maintained in the furnace by adjusting a damper (7) on the exhaust port. The exhaust port is also connected to a variable speed fan that could be used to balance pressures within the furnace.

Instrumentation was provided to monitor furnace conditions (i.e., furnace temperature, pressure, and heat flux) as well as containers conditions (i.e., wall temperatures and heat flux on the outside of the container. Data were collected at a rate of 1 Hz using a National Instruments SCXI-1000 data acquisition chassis with one SCXI-1303, 32-channel isothermal terminal block, and one SCXI-1327, 8-channel high-voltage attenuator terminal block. The National Instruments hardware was interfaced with Labview 8.1 data acquisition software using a 16-bit PCMCIA converter.

Temperature measurements were made on the center of the inside walls of the PA-124 surrogate with Type K, 0.125-in Inconel-sheathed, ungrounded thermocouples. Five thermocouples were used to measure the wall temperature on each internal face except for the top (lid). Adiabatic temperatures were also determined by measuring the temperatures of the four PTs placed externally to the test surrogate. Furnace temperatures were measured at four locations surrounding the containers and averaged. Type K, Inconel-sheathed thermocouples, as specified in UL 1709, were placed throughout the furnace to determine the temperature and track to the prescribed UL 1709 temperature/time curve shown in figure 16.

The heat flux inside of the furnace was measured using a water-cooled, Schmidt Boelter type heat flux transducer with a range of 0–200 kW/m^2. Incident heat-flux measurements were collected from the transducer when mounted in the wall of the furnace. The heat flux from the furnace exposure was monitored for coincidence with the time/heat flux curve, as specified by UL 1709 shown in figure 17, and to provide a comparison to the data calculated from the plate thermometer measurements.

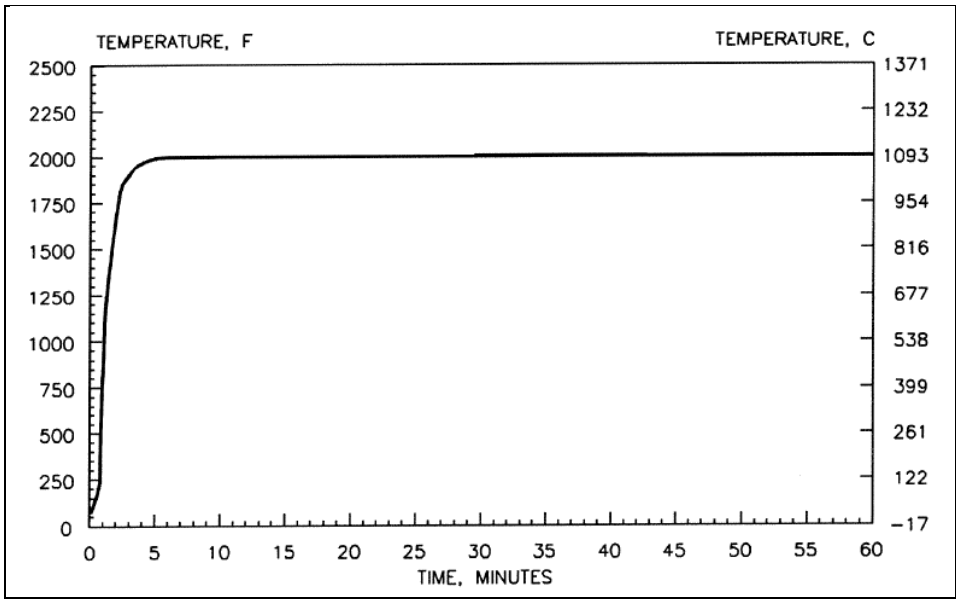

Figure 16. Furnace time/temperature curve as specified by UL 1709 (*6*).

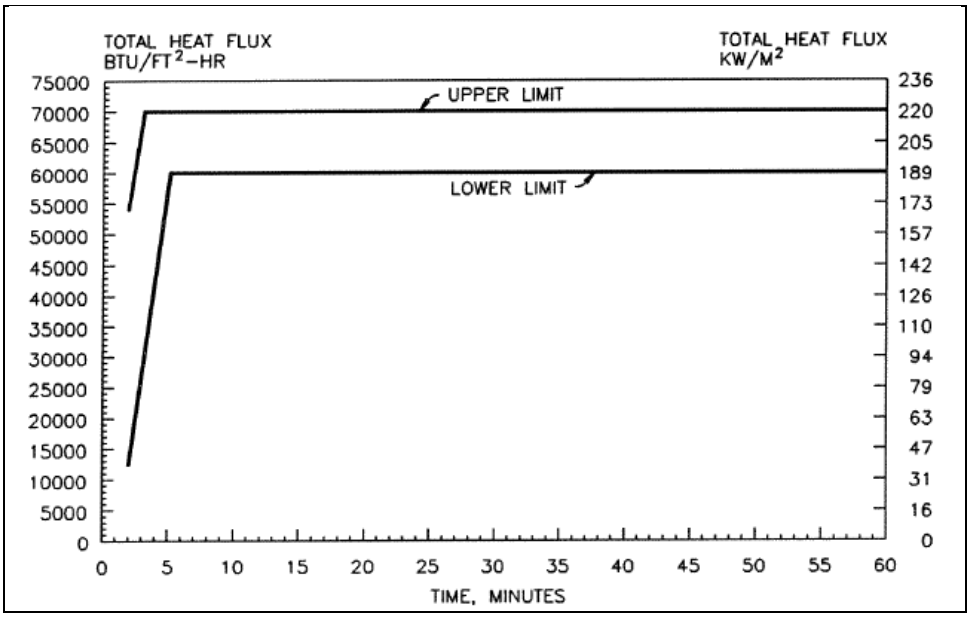

Figure 17. Furnace time/total heat flux curve as specified by UL 1709 (*6*).

3.2 Furnace Exposure Results and Analysis

Five 20-min-long, UL 1709 furnace tests were conducted, with the Δ-container being tested three times and the X-container two times. In general, the furnace exposures for these tests were found to be very repeatable. The average furnace temperatures and heat fluxes for the testing performed on both containers are shown in figure 18. These temperature and heat-flux trends are compared to the curves prescribed in the UL 1709 standard.

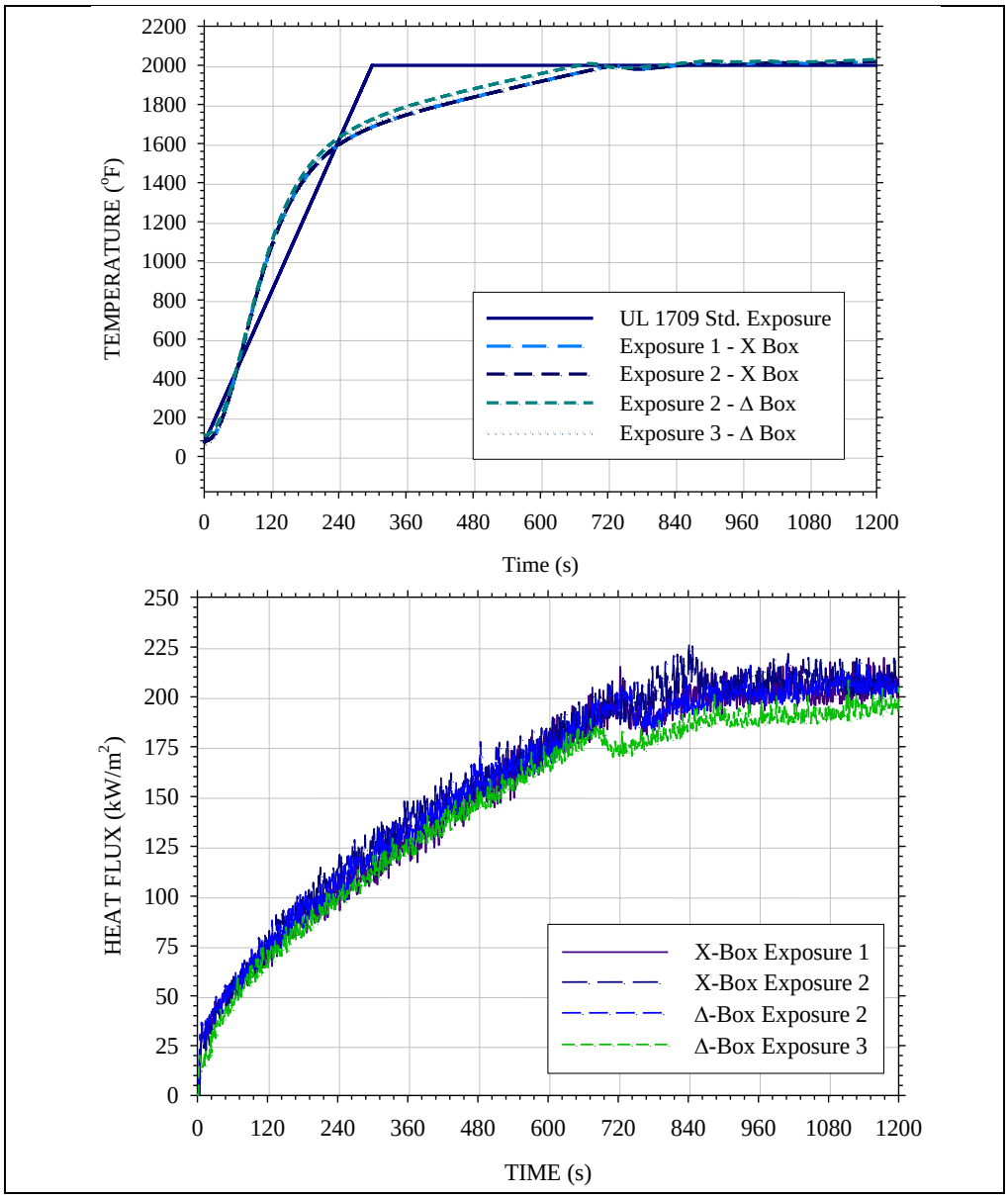

Figure 18. Average temperatures and heat fluxes during furnace testing of both X and Δ containers.

The furnace was not capable of increasing to 1093 °C (2000 °F) as rapidly as prescribed by UL 1709 for any test. In all tested cases, the furnace took ~10–12 min to reach the steady state temperature, which is longer than that specified in UL 1709. However, given that the purpose of these tests is to verify and calibrate the measurements collected by the instrumented container against the Schmidt-Boelter heat-flux transducer, strict adherence to the test standard is not essential. In general, the tests showed excellent consistency in temperature exposure between all runs. The heat fluxes tested were slightly higher during testing of the X container than during the Δ container, but both fell within the prescribed limits once steady state was achieved. The average temperature profiles for both the X and Δ containers are shown in figure 19.

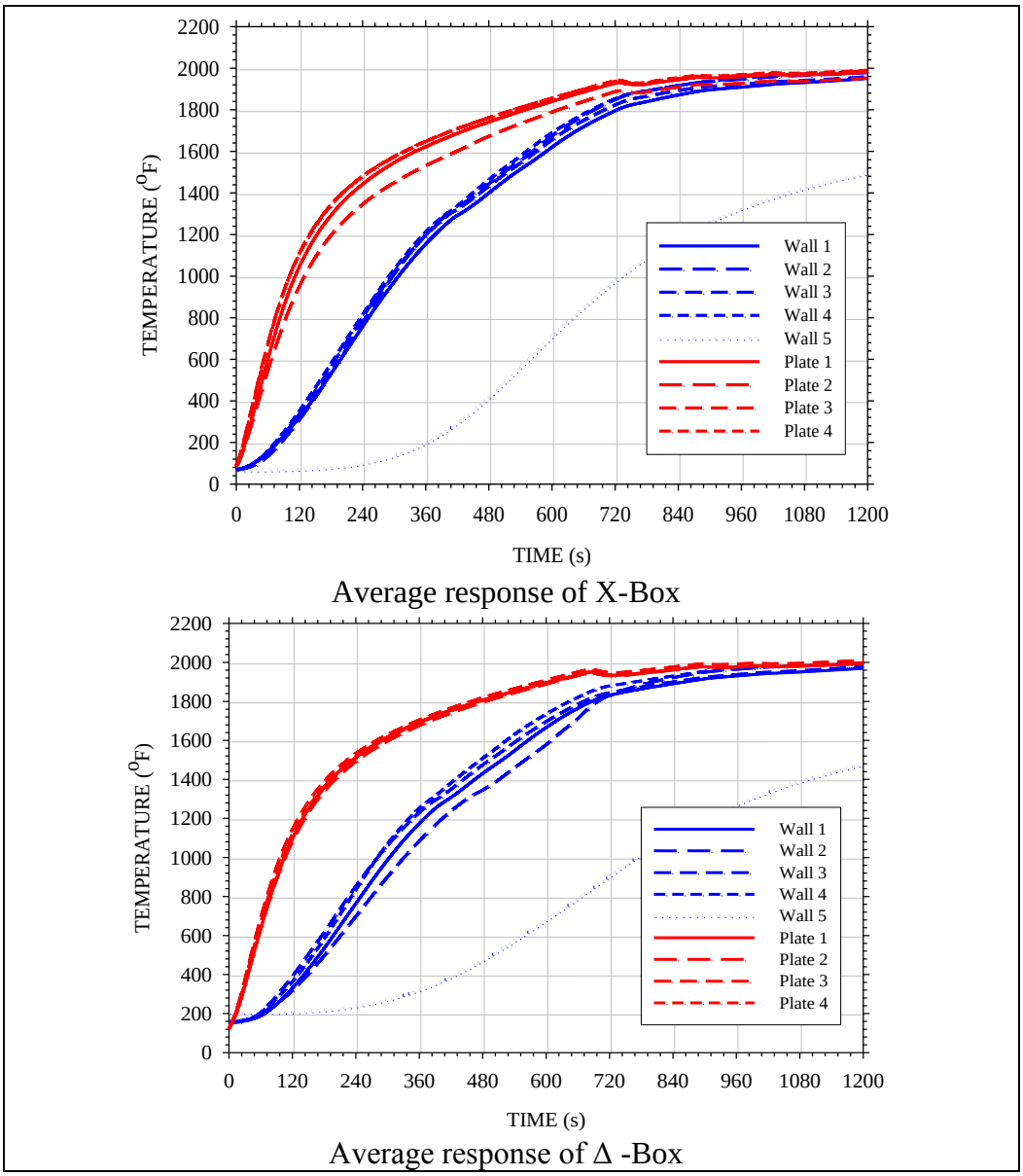

Figure 19. Instrumented container and plate thermometer temperatures during furnace exposure.

The PTs for each test show excellent uniformity in temperature profiles. Each plate within the furnace shows similar thermal response despite their orientation, thus the uniformity of heating within the test furnace can be assumed. The PTs also showed excellent repeatability between subsequent tests. It should be noted, however, that some flaking of layers of the steel container were seen after each conducted exposure test. The results of subsequent tests did not demonstrate a significant change in the thermal response. However, it should be noted that the containers will only survive a finite number of tests before flaking has significantly degraded the wall thickness. The PTs attached to each separate test container also display good consistency between the heating profiles of each surrogate container.

The container walls also demonstrate excellent consistency between all four exposed surfaces and between the two test surrogates. The fifth side of the container is resting upon the insulated shelf within the furnace, and thus experiences a much slower temperature rise. This temperature profile also shows excellent reproducibility between the test containers. It should be noted that both containers experience a slight inflection in the temperature profile near the Curie point. This appeared to be consistent during all tests and for all sides of the wall. While a fairly non-profound change in the surface temperature occurs, the inflection results in significant changes to the storage term in the calculation of heat flux by equation 5, including creating a large spike in the calculated heat flux when passing through the Curie temperature.

The calculated heat fluxes from each surface, and averaged over all tests, are shown for the X-container in figure 20 and for the Δ-container in figure 21. In general, good agreement is demonstrated between the test samples and the Schmidt-Boelter type heat flux gauge within the furnace. The large, short spikes indicate that the temperature has passed through the Curie temperature. The linear regression coefficient (r) was calculated for each container surface and plate thermometer with regard to the measured heat flux. The PTs show better agreement than the container surfaces, as to be expected due to the plate thickness, with an average coefficient of 0.991. The four exposed container surfaces have an average correlation coefficient of 0.945. Wall 5 (bottom) of each container was resting upon insulation and was not exposed to the furnace heat flux and thus shows poor correlation.

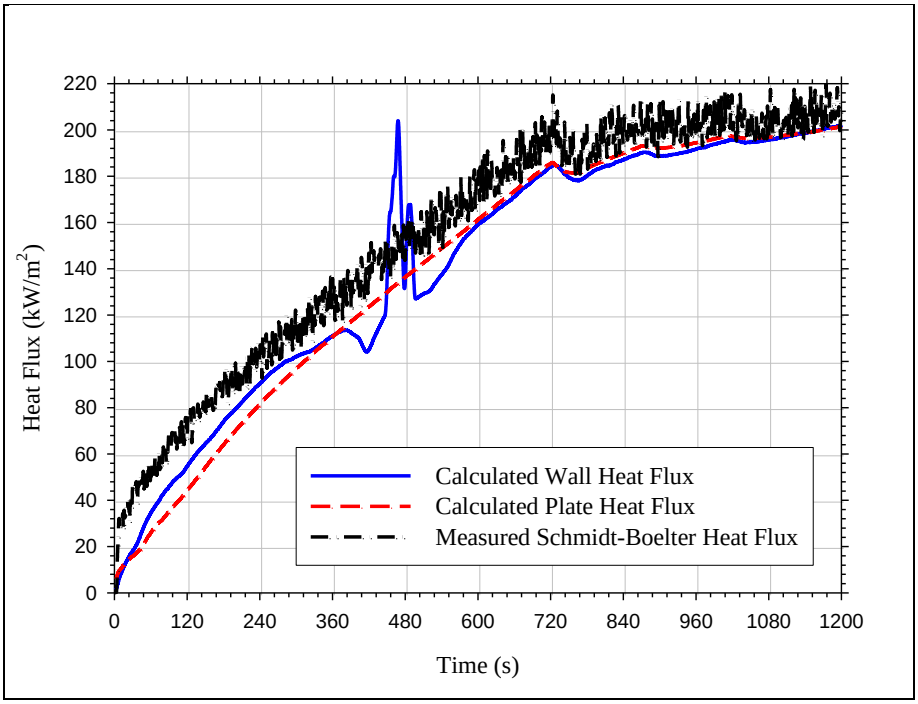

Figure 20. Comparison of measured and calculated heat fluxes taken during X-box furnace tests.

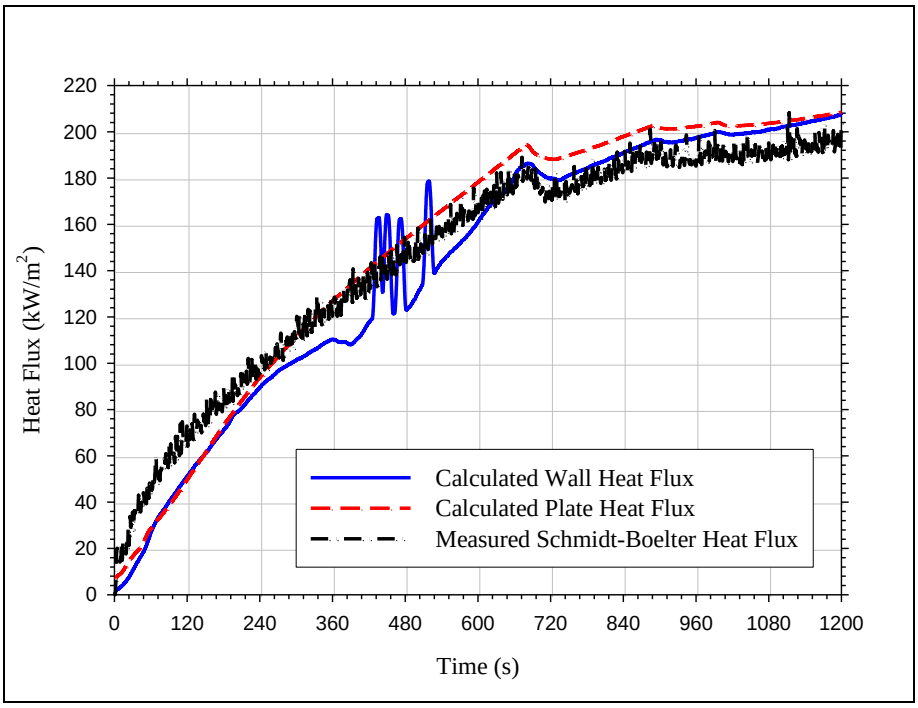

Figure 21. Average calculated heat fluxes from individual container surfaces and PTs during Δ-container furnace tests.

Steady state values in the Δ-container generally show better agreement with the measured heat flux, while the X-container achieves slightly lower than measured values. It should be noted, however, that the furnace temperatures, sample temperatures, and sample heat fluxes were nearly identical for tests conducted with both containers, but the measured heat fluxes were generally higher during the X-container testing. It is unclear whether this is an artifact of the heat flux gauge or a real phenomenon occurring between testing of the two container samples.

All exposed surfaces within the furnace generally demonstrated uniform results. The thermal exposure within the furnace is expected to provide a uniform heat flux, and thus the container constructions are shown to demonstrate reproducibility both between individual surfaces within each construction, between subsequent tests of each construction, and between unique surrogate constructions. The average calculated heat fluxes for all container walls through all tests for each surrogate container are shown in figure 22, with the linear regression coefficient for each data set displayed.

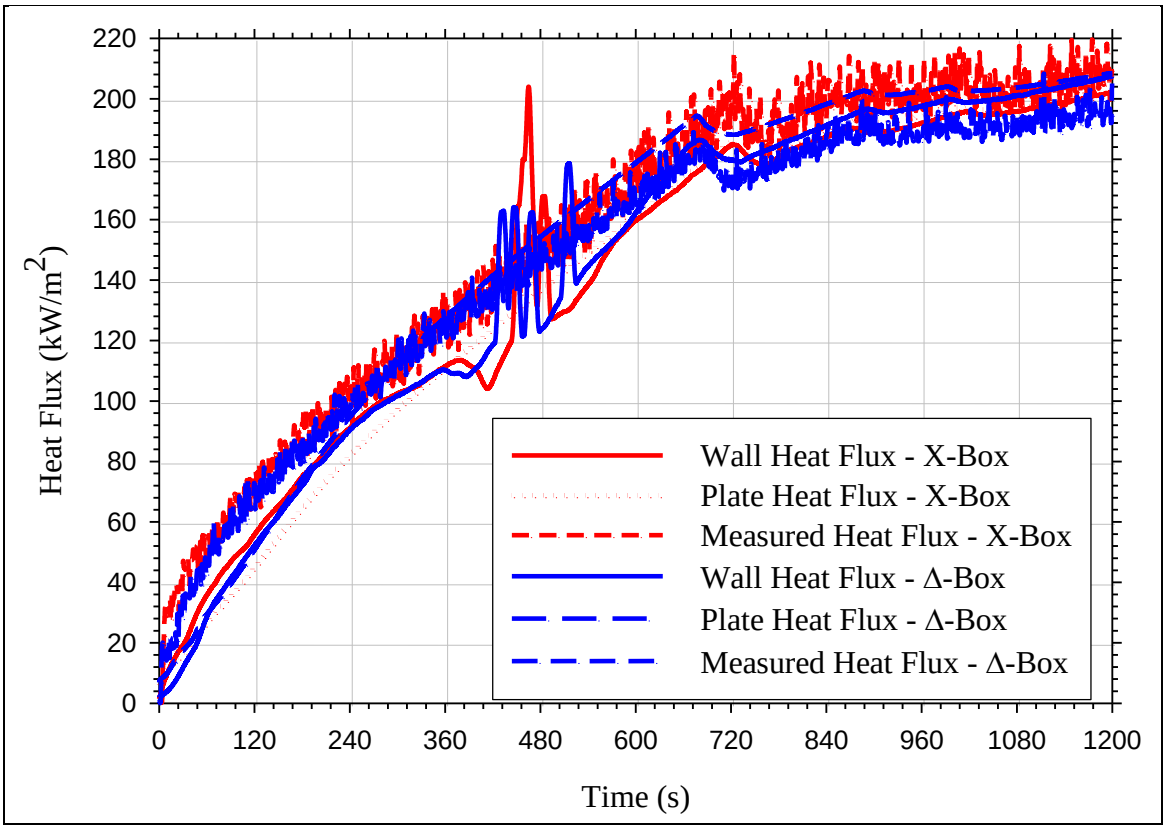

Figure 22. Average calculated heat fluxes from all container surfaces and PTs on the X-container and Δ-container for over all tests.

3.3 Calibration of Instrumented Test Article

The surrogate containers have been shown to both survive fire exposures with minimal thermal degradation and provide accurate estimates of thermal heat flux exposure. The UL 1709 furnace exposure proved to be a simple and repeatable exposure test for applying rapidly increasing heat flux exposure to the instrumented containers. The samples were constructed as instrumented replicas of the PA-124 munitions container with external plate thermometers and responded to the exposures with consistency and reproducibility between two separate surrogate constructions.

The methods of Ingason and Wickstrom (*9*) were shown to produce an accurate method for calculating the incident radiative heat flux on the PTs and the container surfaces. The measured surface temperatures were used in simple calculations and shown to measure the incident heat fluxes with a level of accuracy, demonstrating a linear relationship between calculated and actual heat fluxes with average regression coefficients (r) of 0.945 for the container surfaces and 0.991 for the plate thermometers. The PTs were shown to provide the best estimate of radiant heat flux. This will allow for estimates of incident heat fluxes to be made during future exposure testing where installation of heat flux gauges is not possible, such as during large pool fires.

Additional heat flux calculation accuracy could be obtained by obtaining more accurate thermal properties of the Inconel PTs and of the carbon steel container. Specifically, estimates of specific heat capacity could be particularly useful, as the temperature response of the container material demonstrated a consistent inflection near 667 °C (1250 °F) that resulted in significant error in the transient calculated heat flux from those surfaces.

Based upon the results of this task, the containers are considered calibrated and robust and will be used to characterize the thermal exposures generated during the liquid fuel/external fire test prescribed in STANAG 4240.

4. Phase III – Characterization of STANAG 4240 Exposure

In order to characterize quantitatively the thermal exposure generated by the STANAG 4240 liquid fuel/external fire exposure, the instrumented container was immersed within the pool fire as required by the test method. Simply measuring temperature and heat flux within the pool fire was deemed insufficient in this work given that the presence of the object, in this case the instrumented container, can change the energy distribution within the fire. Since the goal of this effort was to develop a test protocol suitable for any munition or weapon system, the containers used were designed to be representative but not identical to an existing system.

In this phase, the instrumented containers described in the previous sections will be used. The container was used to characterize the thermal exposure resulting from the STANAG 4240 fire. This test article was designed for survivability such that it could be re-used for multiple test configurations and was instrumented specifically to characterize the heat flux incident to the various walls of the container. The data collected in these tests was compared to data obtained from UL 1709 furnace exposures conducted in the previous task and will be compared to other fire exposure scenarios.

4.1 STANAG 4240 Fire Exposure

The fires used in this task were in general accordance with the requirements of STANAG 4240. All tests were conducted above a 2.2- × 2.2- × 0.3-m (7.1- × 7.1- × 1.0-ft) steel pan using 208 L (55 gal) of JP-5 fuel. A photograph of the fuel pan as used in this task is provided in figure 23.

As shown in figure 23, the fuel pan was located on the concrete mini deck at the Chesapeake Beach Detachment Facility in Chesapeake Beach, MD. The container was suspended between two nominally 2.0 m (80 in) tall concrete block pillars in the center of the pan. A single section of 6.35-mm (0.25-in)-thick, 76.2-mm (3-in) angle iron was used to span the block towers. Two sections of stainless steel chain were suspended from the angle iron and attached to the container. All of the support structure was wrapped in a single layer of 25.4-mm (1-in)-thick ceramic fiber to prevent thermal degradation during the fire exposure. The instrumented container was

suspended ~0.36 m (14 in) above the initial surface of the fuel for all tests. A schematic of the test setup is provided in figure 24 showing pan dimensions and distances between the edge of the pan and boundaries of the container.

Figure 23. Photograph of steel fuel pan with instrumented container in place.

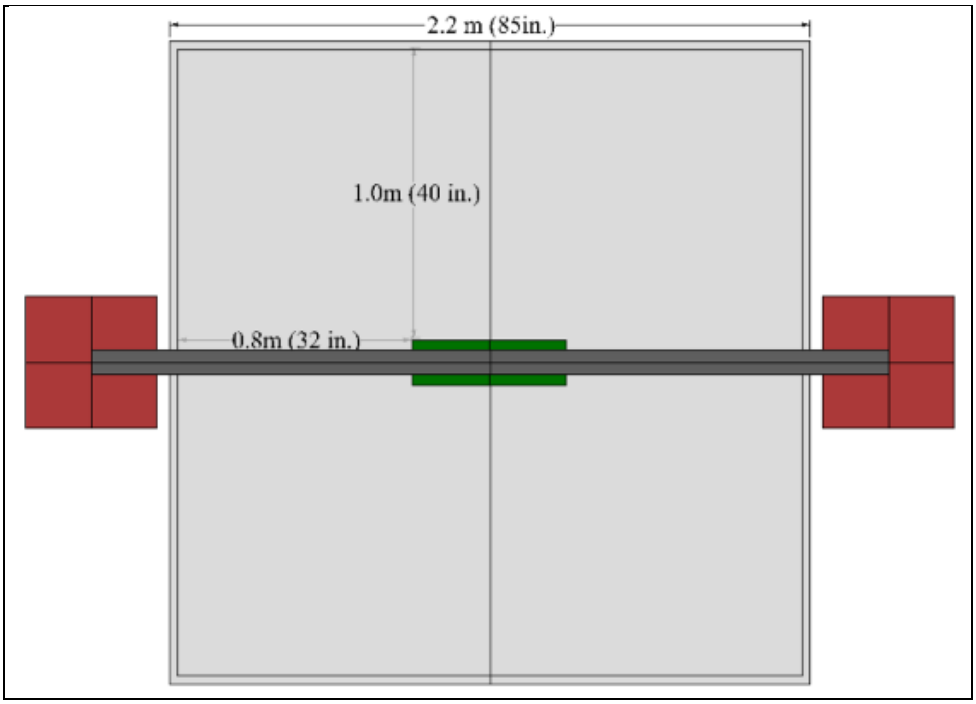

Figure 24. Plan view of test setup showing container location within fuel pan.

Using the fuel properties of JP-5 shown in table 1 and in combination with the calculations of equations 11–14, the approximate fire size was calculated and is also presented in table 3 (*12*).

Table 3. JP-5 fuel properties and calculated test fire characteristics.

Fuel	**Mass Burning Rate m" (kg/m^2-s)**	**Heat of Combustion $\Delta H_{c,eff}$ (kJ/kg)**	**Density ρ(kg/m^3)**	**Empirical Constant kb (m-1)**
JP-5	0.054	43,000	810	1.6
Flame Properties	**Heat Release Rate Q (kW)**	**Burn Duration t_b (min)**	**Flame Height**	
			L_f (m)	**L_f (ft)**
	10,565	11.21	6.68	23.2

$$D = \sqrt{\frac{4A_{Dike}}{\pi}} \ , \tag{11}$$

$$Q = \dot{m}''_{\infty} \Delta H_{c,eff} (1 - e^{-k\beta D}) A_{Dike} \ , \tag{12}$$

$$t_b = \frac{4V\rho}{\pi D^2 \dot{m}''} \ , \tag{13}$$

and

$$L_f = 0.235Q^{2/5} - 1.02D \ , \tag{14}$$

where D = effective pool diameter, A_{dike} = the area of the fuel pan, V = the volume of fuel, and Q = heat release rate.

In order to achieve the fire growth rate specified in STANAG 4240, the ignition and flame spread rate of the JP-5 pool was enhanced using 3.8 L (1 gal) of gasoline, which was floated on the surface of the fuel. Applying the same calculations to the gasoline, an additional 1 min of burn duration was added to the beginning of the test, with a slightly higher (9.5 MW vs. 9.0 MW) heat release rate. The gasoline ignition fire estimate is summarized in table 4 (*12*).

Table 4. Gasoline fuel properties and calculated flame characteristics.

Fuel	**Mass Burning Rate m" (kg/m^2-s)**	**Heat of Combustion $\Delta H_{c,eff}$ (kJ/kg)**	**Density ρ (kg/m^3)**	**Empirical Constant kb (m-1)**
JP-5	0.055	43,700	740	2.1
Flame Properties	**Heat Release Rate Q (kW)**	**Burn Duration t_b (min)**	**Flame Height**	
			L_f (m)	**L_f (ft)**
	11,097	0.18	6.87	19.6

The fuel was ignited locally using a propane torch attached to a stick. The STANAG calls for the use of a bag of powdered charge placed in multiple locations in the pool, but the gasoline provided quick flame spread across the entire pool surface. A photograph of the STANAG 4240 exposure fire created for these tests is provided in figure 25.

Figure 25. Representative photograph of STANAG 4240 exposure fire characterized in this task.

4.2 STANAG 4240 Exposure Results and Analysis

Instrumentation was provided to monitor pool fire flame temperatures, container wall temperatures, and container plate thermometer temperatures. Data were collected at a rate of 1 Hz using a using a National Instruments SCXI-1000 data acquisition chassis with one SCXI-1303, 32-channel isothermal terminal block. The National Instruments hardware was interfaced with Labview 8.1 data acquisition software using a 16-bit PCMCIA converter.

Temperature measurements were made at the center of the inside walls of the PA-124 surrogate with Type K, 1/8-in Inconel sheathed, ungrounded thermocouples. Five thermocouples were used to measure the wall temperature on each internal face except for the top (lid). In addition, flame temperatures were taken at three locations surrounding the tested surrogate. Type K, Inconel sheathed thermocouples were placed port, starboard, and aft of the test surrogate in a horizontal plane passing through the center of the surrogate. They were placed 50 mm (2 in) from the external walls of the container. The external flame temperature thermocouples are shown with the surrogate supported on the chain mount in figure 26.

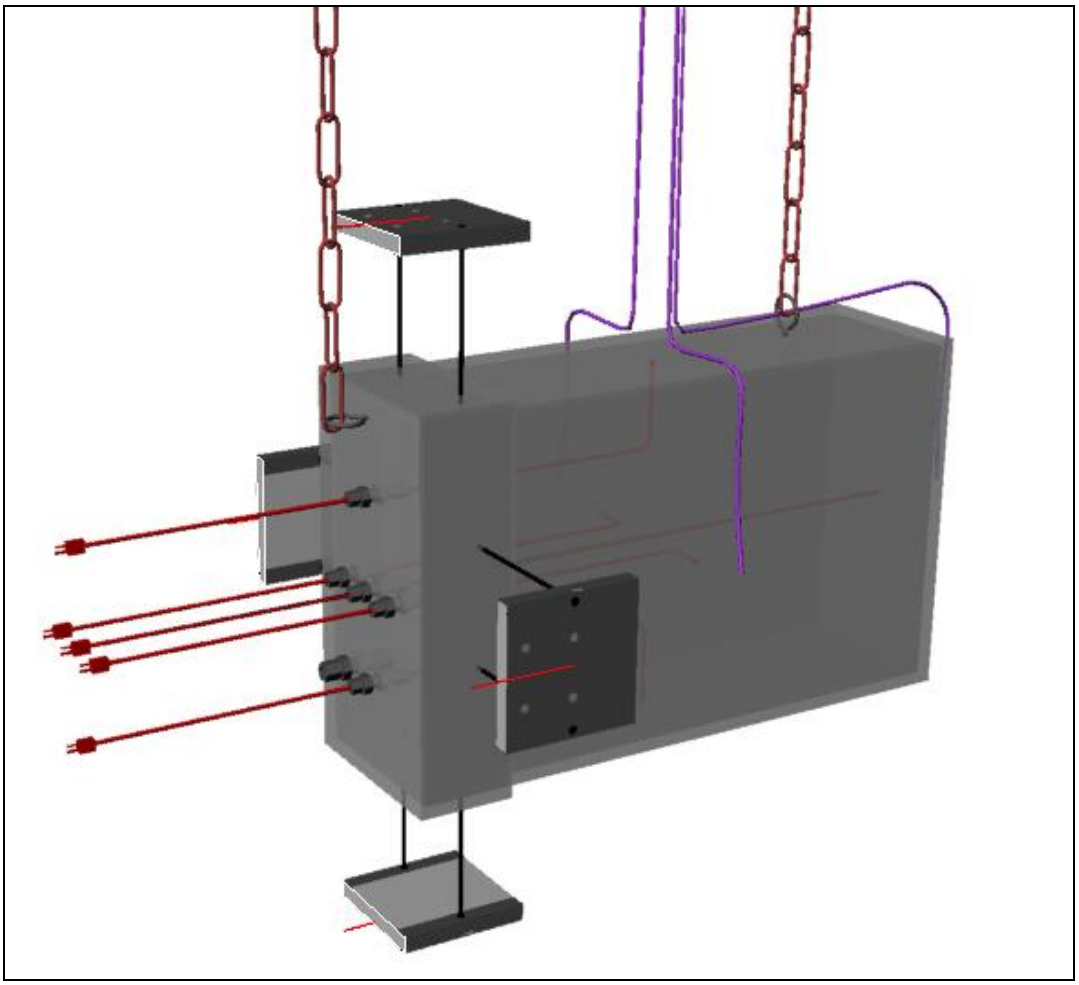

Figure 26. External flame temperature measurement locations.

All tests were conducted in accordance with the guidelines of STANAG 4240. The exact procedures followed for each test are outlined in this section. All thermocouples were connected and verified operational by the DAQ system. Once verified, 208 L (55 gal) of JP-5 was poured into the fuel pan to an initial depth of 5 cm (2 in); 3.8 L (1 gal) of regular, unleaded gasoline was then poured into the fuel pan. All personnel retreated to a safe distance, and when the area had been cleared, data acquisition and video recording began. One minute of background data was obtained, and then the pool was ignited using the stick torch. The exposure fires were considered active once two of the external thermocouples recorded a temperature of 550 °C (1022 °F). The tests were considered to meet the standards for exposure under STANAG 4240 when the average of the external thermocouples had reached 800 °C (1472 °F). The exposures continued until all fuel had been consumed. Data acquisition and video recording continue for 1 min after the flames had self-extinguished.

Four replicate tests were conducted using the same container. In general, the tests produced repeatable results and provided a large data set to which comparisons can be made in future efforts toward building a gaseous fuel equivalency test. In general, the tests produced similar exposures, as measured by the container, and were conducted under generally similar conditions. A summary of the fire exposure duration and average ambient conditions during this exposure is provided in the following sections as well as in table 5.

Table 5. Summary of test conditions for STANAG 4240 testing.

Test No.	Flame Duration (min)	Ambient Temperature (°C [°F])	Average Wind Speed (kph [mph])	Time After Ignition That Temperature at Two Locations Is >550 °C (1022 °F) [s]	Time After Ignition That Mean Temperature at All Locations Reaches 800 °C (1472 °F) [s]	Average Flame Temperature (°C [°F])
1	15	21 [70]	5.8 [3.6]	35	77	697 [1286]
2	12	22 [72]	5.3 [3.3]	13	30	714 [1317]
3	11	24 [76]	2.9 [1.8]	17	30	687 [1268]
4	11	24 [76]	5.3 [2.3]	24	28	763 [1406]

4.2.1 Test 1

In the first liquid fuel/external fire test, the JP-5 fuel was poured directly into the test pan without adding a water sub-layer. The absence of the water sub-layer in this test resulted in the pan bowing up in the center due to thermal stresses within the steel. This bowing of the pan caused the fuel to preferentially burn at the edges, with no significant burning in the center later in the test. A photograph of the bowing of the center of the pan and the preferential burning around the perimeter of the pan is provided in figure 27.

Figure 27. Photograph of condition of pan after test no. 1 conducted without water sub-layer present.

Despite the warping of the fuel pan, the container was immersed in the fire plume for the majority of this test. Thus, the data from this test was considered and included in the analysis performed in this task. Plots of the average flame temperatures, calculated wall heat fluxes, and calculated plate heat fluxes are presented in figure 28.

In test 1, an average wind speed of 5.8 kph (3.6 mph) was measured during the exposure. An average flame temperature of 550 °C (1022 °F) was reached 35 s after ignition. Per the requirements of STANAG 4240, this time will be denoted as time zero for this test for all future discussion. The 800 °C (1472 °F) threshold specified in STANAG 4240 was achieved 42 s after time zero. The average flame temperature dropped below 550 °C (1022 °F) 711 s after time zero. This will be considered as the end of the exposure for all calculations. The average flame temperature measured during the exposure was 697 °C (1286 °F). As shown in figure 28, the measured flame temperatures were very comparable between each location. A summary of the average and maximum calculated heat fluxes measured during this test exposure is presented in table 6. It should be noted that the average heat fluxes reported in table 6 were calculated between the time that any two of the fire temperature measurements exceeded 550 °C (1022 °F) to the time any two of the fire temperature measurements fell below this temperature. The 550 °C (1022 °F) temperature threshold was adopted based upon the procedures outlined in STANAG 4240 for the timing of hazardous events (*2*).

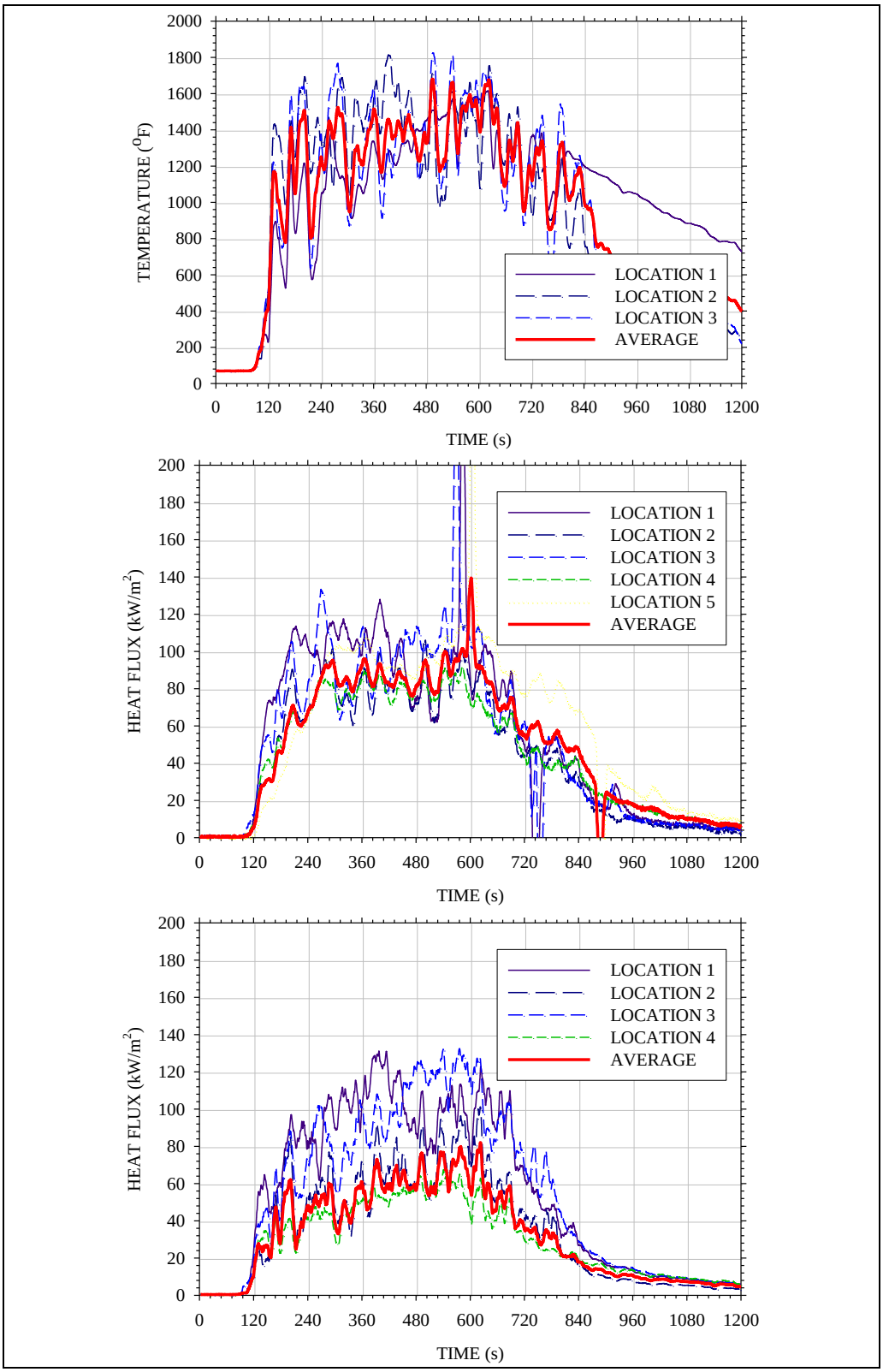

Figure 28. Plot of flame temperatures (top), calculated wall heat flux (bottom left), and calculated plate heat flux (bottom right) measured in test 1.

Table 6. Summary of heat flux data collected during STANAG 4240 test 1.

Measurement Type	Measurement Location	Avg. Heat Flux (kW/m^2)	Peak Heat Flux (kW/m^2)
Wall	1	97	128
	2	80	107
	3	96	133
	4	79	90
	5	94	109
Plate	1	101	131
	2	61	94
	3	95	127
	4	50	65
Exposure to Walls		**89**	**128**
Exposure to Plates		**77**	**131**

As shown in table 6, the calculated heat fluxes on the vertical faces of the container (i.e., the faces of the container that were perpendicular to the fuel surface) were consistently higher than those measured on surfaces parallel to the fuel surface (i.e., topside and fire side). On average, the vertical face heat fluxes were 16 kW/m^2 greater than those measured on horizontal surfaces when using the wall heat fluxes and 42 kW/m^2 greater when using plate surfaces. The average heat flux exposure to the instrumented container in this test was 89 kW/m^2 as measured on the walls and 77 kW/m^2 as measured on the plate thermometers.

4.2.2 Test 2

The second liquid fuel/external fire test was conducted with a 50.8-mm (2-in) deep water sub-layer to prevent warping of the pan and maintain a flat fuel surface. In this test, the JP-5 fuel was poured directly onto the water sub-layer, spiked with gasoline, and ignited. In general, the fire exposure in this test was more uniform and more consistently engulfed the container than in the previous test (test 1). This was most likely the result of the fuel layer remaining constant of the entire area of the fuel pan. In this test, the average wind speed over the duration of the exposure was 5.3 kph (3.3 mph). A photograph of the fire exposure generated in test 2 is provided in figure 29.

In this test, an average flame temperature of 550 °C (1022 °F) was reached 13 s after ignition. Per the requirements of STANAG 4240, this time will be denoted as time zero for this test in all future discussions. The 800 °C (1472 °F) threshold specified in STANAG 4240 was achieved in 16 s after time zero. The average flame temperature dropped below 550 °C (1022 °F) 601 s after time zero. This will be considered as the end of the exposure for all calculations. The average flame temperature measured during this test was 706 °C (1303 °F). This value is very similar to that measured in test 1. A summary of the various calculated heat fluxes measured during this test is presented in table 7. Average flame temperatures, calculated wall heat fluxes, and calculated plate heat fluxes measured in this test are presented in figure 30.

Figure 29. Representative photograph of fire exposure generated during test 2.

Table 7. Summary of heat flux data collected during STANAG 4240 test 2.

Measurement Type	**Measurement Location**	**Avg. Heat Flux (kW/m^2)**	**Peak Heat Flux (kW/m^2)**
Wall	1	94	137
	2	74	128
	3	78	118
	4	70	94
	5	84	140
Plate	1	94	140
	2	59	121
	3	77	126
	4	50	77
Exposure to Walls		**80**	**140**
Exposure to Plates		**70**	**140**

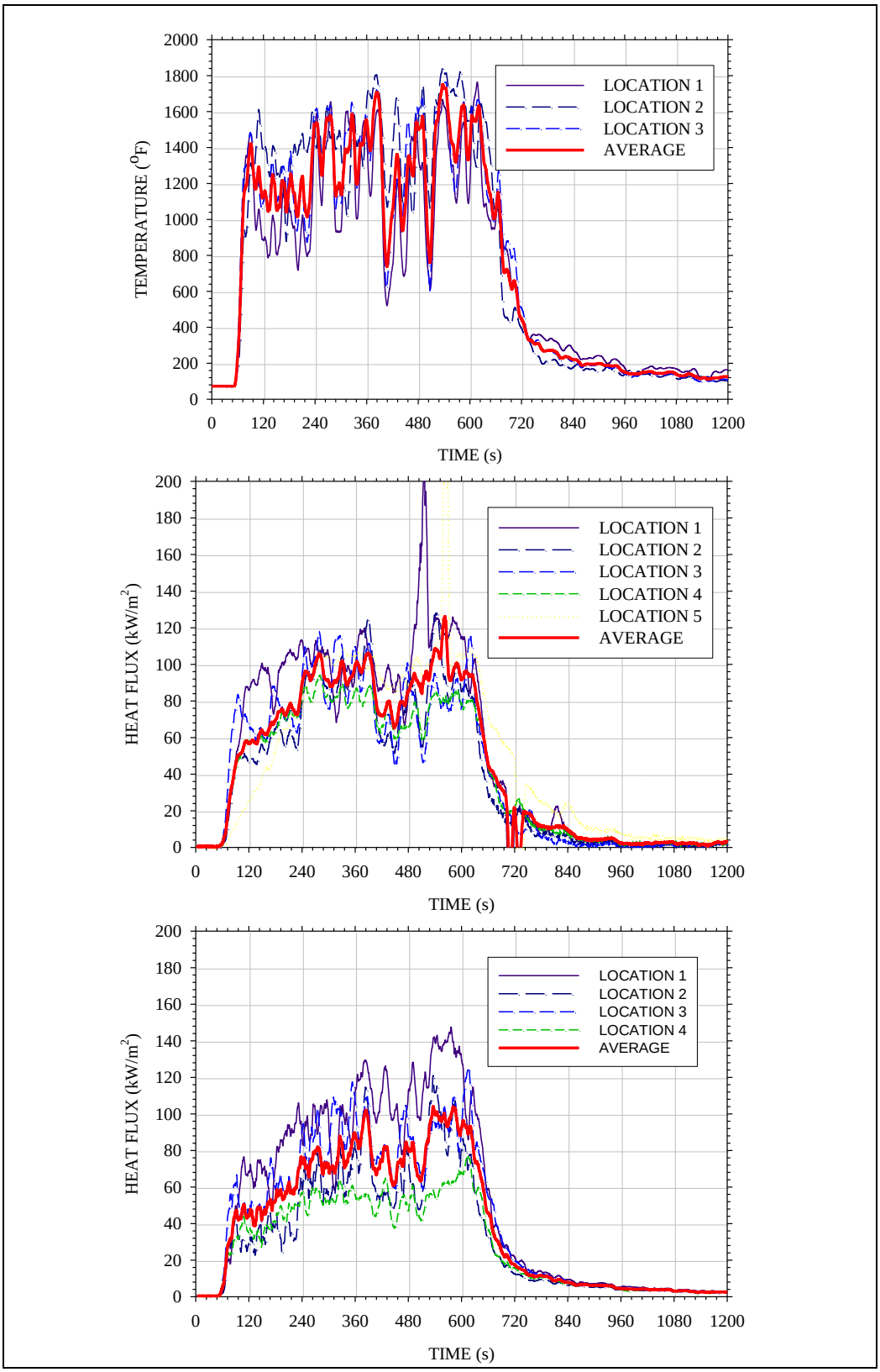

Figure 30. Plot of temperatures (top), calculated wall heat flux (bottom left), and calculated plate heat flux (bottom right) measured in test 2.

As shown in table 7, the calculated heat fluxes on the vertical faces of the container (i.e., the faces of the container that were perpendicular to the fuel surface) were consistently higher than those measured on surfaces parallel to the fuel surface (i.e., topside and fire side). On average, the vertical face heat fluxes were 13 kW/m^2 greater than those measured on horizontal surfaces when using the wall heat fluxes and 31 kW/m^2 greater when using plate surfaces. The average heat flux exposure to the instrumented container in this test was 80 kW/m^2 as measured on the walls and 70 kW/m^2 as measured on the plate thermometers.

4.2.3 Test 3

The third liquid fuel/external fire test was conducted using the exact same approach as described for Test 2 (i.e., with a 50.8-mm [2-in] deep water sub-layer). In this test, the JP-5 fuel was poured directly onto the water sub-layer, spiked with gasoline, and ignited. The fire exposure was generally similar to that observed in test 2. In this test, the average wind speed over the duration of the exposure was 2.9 kph (1.8 mph). A photograph of the fire exposure generated in test 3 is provided in figure 31.

In this test, an average flame temperature of 550 °C (1022 °F) was reached 16 s after ignition. Per the requirements of STANAG 4240, this time will be denoted as time zero for this test in all future discussions. The 800 °C (1472 °F) threshold specified in STANAG 4240 was achieved in 13 s from time zero. The average flame temperature dropped below 550 °C (1022 °F) 574 s after time zero. This will be considered as the end of the exposure for all calculations. The average flame temperature measured during this test was 689 °C (1273 °F). This value is slightly less than the average flame temperature measured in the first two tests conducted but is still relatively similar. A summary of the various calculated heat fluxes measured during this test is presented in table 8. Average flame temperatures, calculated wall heat fluxes, and calculated plate heat fluxes measured in this test are presented in figure 32.

As shown in table 8, the calculated heat fluxes on the vertical faces of the container (i.e., the faces of the container that were perpendicular to the fuel surface) were consistently higher than those measured on surfaces parallel to the fuel surface (i.e., topside and fire side). On average, the vertical face heat fluxes were 15 kW/m^2 greater than those measured on horizontal surfaces when using the wall heat fluxes and 36 kW/m^2 greater when using plate surfaces. The average heat flux exposure to the instrumented container in this test was 77 kW/m^2 as measured on the walls and 59 kW/m^2 as measured on the plate thermometers.

Figure 31. Representative photograph of fire exposure generated during test 3.

Table 8. Summary of heat flux data collected during STANAG 4240 test 3.

Measurement Type	**Measurement Location**	**Avg. Heat Flux (kW/m^2)**	**Peak Heat Flux (kW/m^2)**
Wall	1	99	133
	2	64	125
	3	68	111
	4	71	86
	5	81	103
Plate	1	96	130
	2	38	95
	3	57	99
	4	45	67
Exposure to Walls		**77**	**133**
Exposure to Plates		**59**	**130**

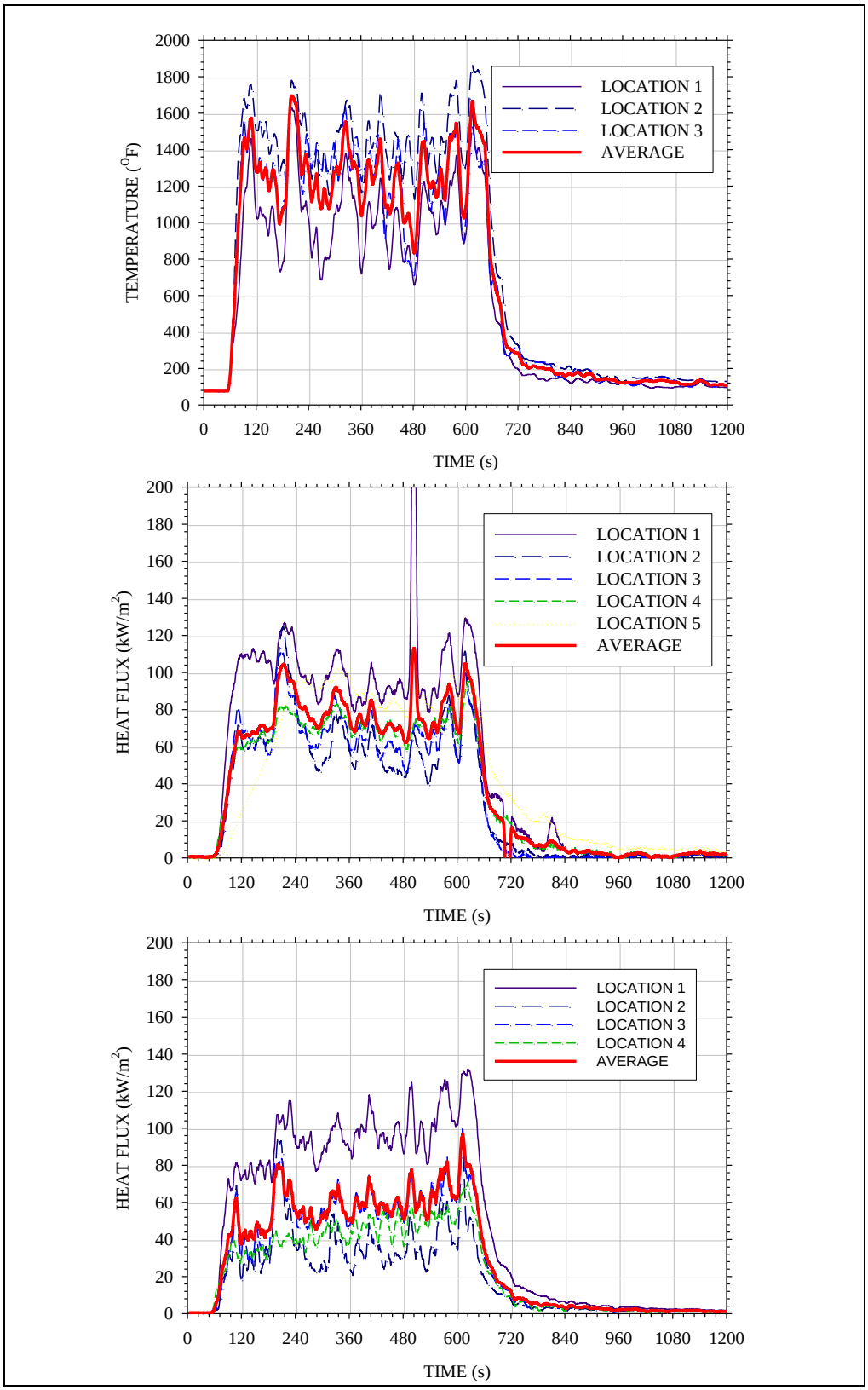

Figure 32. Plot of temperatures (top), calculated wall heat flux (bottom left), and calculated plate heat flux (bottom right) measured in test 3.

4.2.4 Test 4

The fourth liquid fuel/external fire test was conducted using the exact same approach as used in tests 2 and 3 (i.e., with a 50.8-mm [2-in] deep water sub-layer). In this test, the JP-5 fuel was poured directly onto the water sub-layer, spiked with gasoline, and ignited. The fire exposure was generally similar to that observed in all previous tests. In this test, the average wind speed over the duration of the exposure was 5.3 kph (2.3 mph). A photograph of the fire exposure generated in test 4 is provided in figure 33.

Figure 33. Representative photograph of fire exposure generated during test 4.

In this test, an average flame temperature of 550 °C (1022 °F) was reached 23 s after ignition. Per the requirements of STANAG 4240, this time will be denoted as time zero for this test in all future discussions. The 800 °C (1472 °F) threshold specified in STANAG 4240 was achieved in 4 s after time zero. The average flame temperature dropped below 550 °C (1022 °F) 604 s after time zero. This will be considered as the end of the exposure for all calculations. The average flame temperature measured during this test was 763 °C (1406 °F). This value is the highest average flame temperature measured of any test, but the results were still relatively similar to all previous tests. A summary of the various calculated heat fluxes measured during this test is presented in table 9. Average flame temperatures, calculated wall heat fluxes, and calculated plate heat fluxes measured in this test are presented in figure 34.

Table 9. Summary of heat flux data collected during STANAG 4240 test 4.

Measurement Type	**Measurement Location**	**Avg. Heat Flux (kW/m^2)**	**Peak Heat Flux (kW/m^2)**
Wall	1	105	138
	2	93	140
	3	92	140
	4	75	87
	5	92	140
Plate	1	111	140
	2	74	140
	3	88	125
	4	51	62
Exposure to Walls		**91**	**140**
Exposure to Plates		**81**	**140**

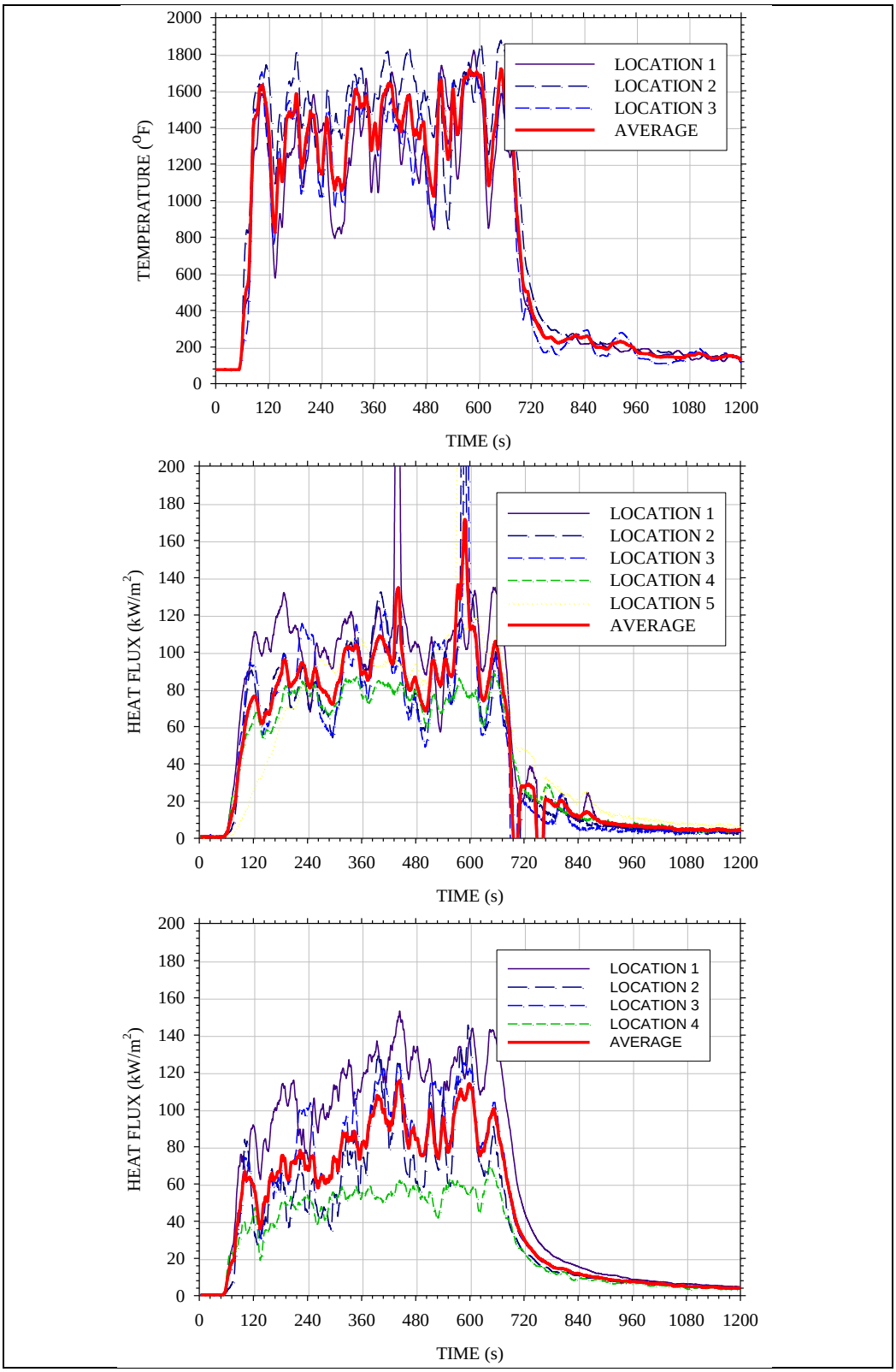

Figure 34. Plot of temperatures (top), calculated wall heat flux (bottom left), and calculated plate heat flux (bottom right) measured in test 4.

As shown in table 9, the calculated heat fluxes on the vertical faces of the container (i.e., the faces of the container that were perpendicular to the fuel surface) were consistently higher than those measured on surfaces parallel to the fuel surface (i.e., topside and fire side). On average, the vertical face heat fluxes were 12 kW/m^2 greater than those measured on horizontal surfaces when using the wall heat fluxes and 37 kW/m^2 greater when using plate surfaces. The average heat flux exposure to the instrumented container in this test was 91 kW/m^2 as measured on the walls and 81 kW/m^2 as measured on the plate thermometers.

4.3 Generalized STANAG 4240 Fire Exposure

Four different STANAG 4240 exposure fires were conducted in a nominally 2-m (6.6-ft) square fuel pan filled with 208 L (55 gal) of JP-5 fuel. The fires burned for an average of 12 min with 2.9–5.8 kph (1.8–3.6 mph) average wind speeds during testing. Average flame temperatures measured in close proximity to the container ranged from 697 to 763 °C (1286–1406 °F), with maximum flame temperatures as high as 978 °C (1792 °F). These thermal exposure data, while being on the low end, are generally consistent with available data for large-scale pool fires. Maximum time-averaged temperatures for pool fires ranged from 770 to 1200 °C (1418–2192 °F). A plot of the average fire temperature profile measured in the STANAG 4240 pool fires conducted is presented in figure 35.

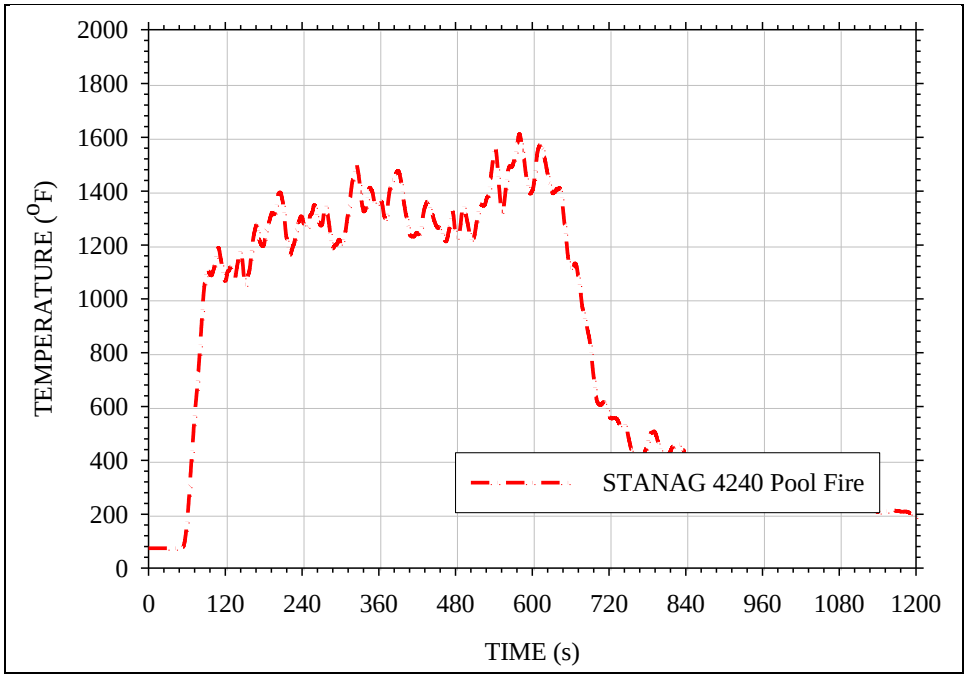

Figure 35. Average STANAG 4240 pool fire exposure temperature.

Under these conditions, the container constructed to be representative of a standard PA-124 munitions container measured average incident heat fluxes ranging from 59 to 91 kW/m^2, depending upon where the measurement was taken, with maximum heat flux values as high as of 140 k/m^2. A summary of the average heat fluxes as measured by the instrumented box during each test is provided in table 10.

Table 10. Summary of heat flux exposure data measured during STANAG 4240 testing.

Measurement Type	**Test ID**	**Avg. Heat Flux (kW/m^2)**	**Peak Heat Flux (kW/m^2)**
Wall	1	89	128
	2	80	140
	3	77	133
	4	91	140
Average STANAG 4240 Exposure at Wall		**84 ± 7**	**135 ± 6**
Plate	1	77	131
	2	70	140
	3	59	130
	4	81	140
Average STANAG 4240 Exposure at Plate Thermometer		**72 ± 10**	**135 ± 6**

The average heat fluxes measured at both the box walls and plate thermometers are presented in figure 36. The average incident heat fluxes measured during these tests were generally lower than those reported in the literature for objects immersed in a pool fire. However, there have been studies (*13*, *14*) that report lower incident heat flux measurements for objects immersed in pool fires where the object size is comparable to that of the pool fire. In these studies (*15*), maximum average heat flux measurements of 75–85 kW/m^2 were reported and attributed to the object reducing the local flame temperatures, thus reducing the thermal insult.

The majority of the time the liquid fuel fires were burning, the container remained immersed in the flame plume. However, at times of extreme wind conditions, the container was exposed to ambient conditions for some period of time. This wind effect coupled with the inherent temperature differences within the fire plume, even under quiescent conditions, resulted in some thermal exposure differences with respect to the orientation of the container. In general, the vertical sides of the container (i.e., sides of the container that were perpendicular to the fuel surface) were subjected to the most severe thermal exposures with the horizontal surfaces being exposed to slightly less severe conditions. On average, the exposures to the vertical surfaces were 10–36 kW/m^2 greater than those measured on the horizontal surfaces.

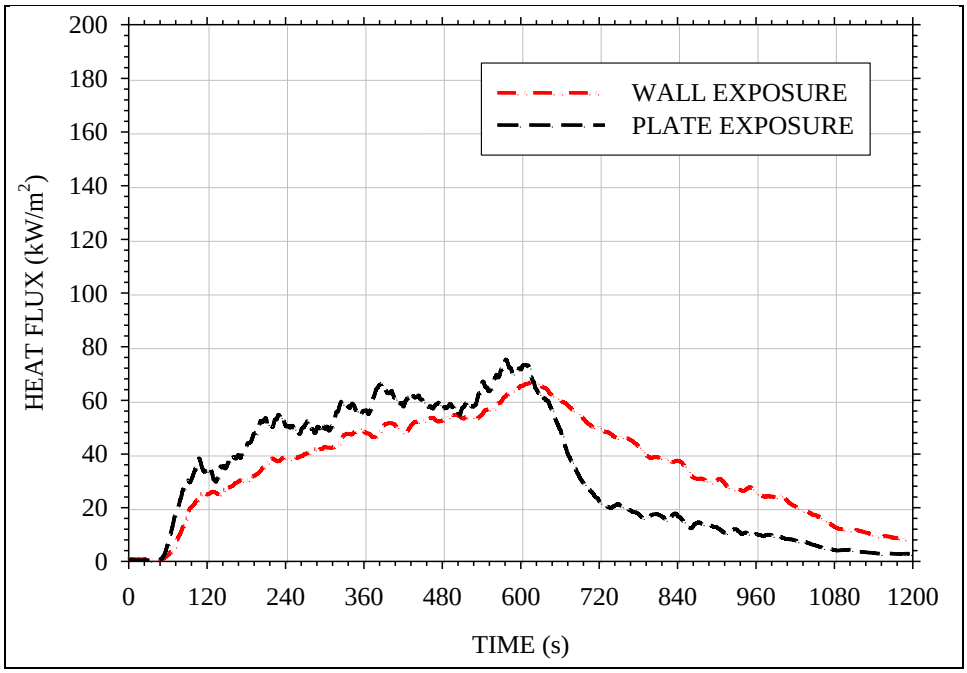

Figure 36. Average STANAG 4240 heat flux exposures.

The data collected in this task characterize the thermal exposure to a container from a STANAG 4240 fire exposure. These data will be used as the baseline to which the thermal exposures generated by several alternative fuel fire exposures will be compared.

5. Phase IV – Development of Alternative Fuel Fire Exposures

The alternative fuel fire exposures discussed in this section were developed to provide a thermal exposure comparable to that of the STANAG 4240 pool fire exposure while, at the same time, providing an additional degree of control and a more environmentally-friendly fire scenario. Liquid and gaseous fuels were identified. A comparison of the fuel properties for the current STANAG 4240 fuel type, as well as the two alternative fuels, is provided in table 11.

Table 11. Comparison of fuel properties.

Fuel	Density (kg/m^3)	Heat of Combustion (MJ/kg)	Soot Yield (g/g)	Radiative Fraction
Jet A (*16*)	806	45.6	0.097 ± 0.016	0.40 ± 0.08
Heptane (*17*)	689	44.5	0.015 ± 0.001	0.46 ± 0.06
Propane (*18*)	1.83	46.0	0.004	0.29 (*16*)

Heptane was selected as the liquid fuel alternative because it represents a liquid fuel with a heat of combustion and radiative fraction comparable to that of current STANAG 4240 fuels, but whose soot yield is ~1/6 that of the STANAG fuels. In addition to the environmental savings from the reduced soot yield, the liquid heptane also reduces the environmental hazards associated with the fuel contacting the ground due to its relatively high volatility and relatively low bio-concentration factor. A full discussion of the environmental benefits of the alternative fuel fires used with respect to the current STANAG 4240 fuels is provided in section 6.

Propane was also selected for evaluation in this test program. Propane is currently being explored as an alternative fuel fire exposure by the international community and was therefore considered in this work. This fuel has combustion properties that are generally similar to that of the current STANAG 4240 fuels, while producing an order of magnitude less smoke. Furthermore, it is a gaseous fuel; thus, the environmental impact of the fuel with respect to ground contamination is minimal as well. However, propane has a radiative fraction that is approximately half that of both the STANAG 4240 fuels and the heptane alternative which could require larger exposure fires to generate an equivalent radiative exposure to an immersed object.

Both of the alternative fuels described, if adopted, would generate fire scenarios that would provide a test facility with substantially more control over the both the ignition and suppression of a fire exposure, thus minimizing the duration of testing and down time between testing.

5.1 Alternative Fuel Fire Exposures

Three different fuel supply systems will be evaluated in this task—two propane-fired systems and one heptanes-fired system. The propane-fired burners will utilize the 227-kg (500-lb) LPG tank located outside the burn building on the U.S. Naval Research Laboratory (NRL) Chesapeake Bay Detachment (CBD) campus. The liquid discharge from the LPG tank will be connected to the inlet side of the Alternate Energy Systems Model AE-40 direct fired vaporizer located in within the burn building. The outlet side of the vaporizer will be connected to a manifold constructed from 25.4-mm (1-in) steel pipe that will be used to feed the propane-fired

burners. The systems will be designed to replicate the exposure generated by the STANAG 4240 liquid fuel/external fire test. Descriptions of the each system to be evaluated are provided in the following subsections.

5.1.1 Heptane Spray Burner

The first fire exposure evaluated was a heptane spray fire system comprised of four vertically oriented Bete P-80 spray nozzles flowing at a rate of ~3.8 l pm (1.0 gpm). The Bete P-80 spray nozzles were installed in a 2 × 2 array with an offset distance of ~1.0 m (3.3 ft) between nozzles. In this orientation, it is expected that the ensuing spray fire would fully engulf the instrumented container suspended above the fuel pan. The heptane spray fire will be supplied using a 303-L (80-gal) fuel reservoir pressurized to ~40 psi. Fuel reservoir pressure was monitored using an Omegadyne PX209-100G5V pressure transducer with a range of 0–100 psi and a resolution of 0.25 psi. The fuel reservoir was pressurized using a high-pressure nitrogen cylinder connected to the reservoir. At 40 psi, given a k-factor of 0.171, each Bete P-80 spray nozzles will provide a flow rate of 1.08 gpm, for a total heptane flow rate of 4.3 gpm. At this flow rate and assuming a combustion efficiency of 0.9, the expected fire size for this test is ~7.4 MW. In this orientation, it is expected that the ensuing spray fire will fully engulf the instrumented container suspended above the fuel pan.

As just indicated, the heptane used during testing was stored in a 303 L (80 gal) fuel reservoir located ~12.2 m (40 ft) from the spray manifold. The fuel reservoir and spray manifold were connected using 12.7-mm (0.5-in) stainless steel tubing. Fuel flow was controlled using a quarter-turn value installed at the base of the fuel reservoir. After leaving the fuel reservoir, the fuel was transported through 12.7-mm (0.5-in) stainless steel tubing and dispersed using the spray manifold shown in figure 37. The nozzles were installed atop 0.1-m (4-in) pipe stems such that the orifice of the nozzle is nominally 0.1 m (4 in) above the base of the fuel pan. During testing, the fuel pan will be filled with a 50.4-mm (2-in) layer of water to mitigate heating/warping of the pan.

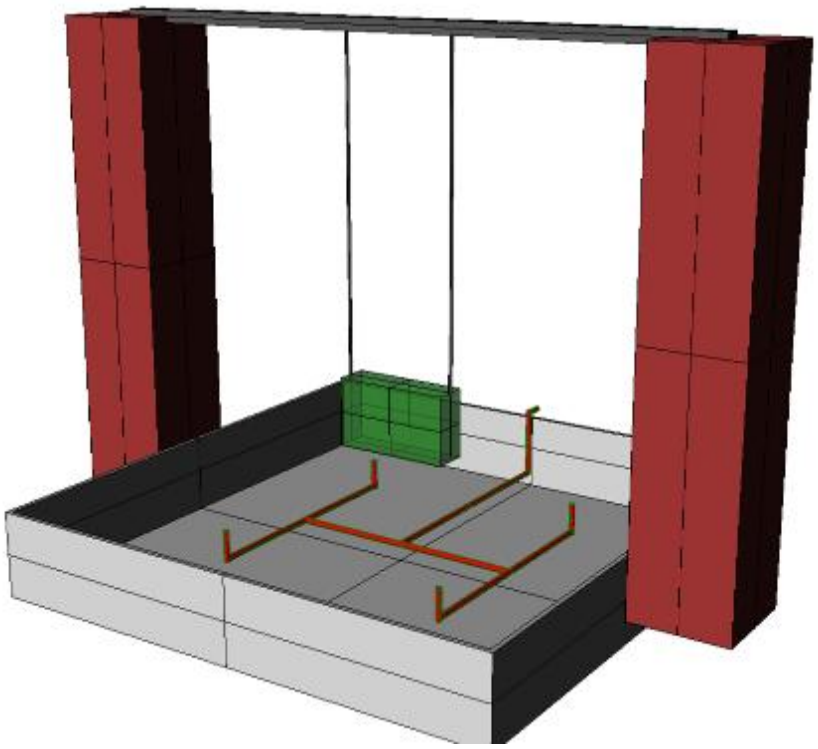

(a) Rendering of heptane spray manifold with nozzles 1 m (3.3 ft) on center.

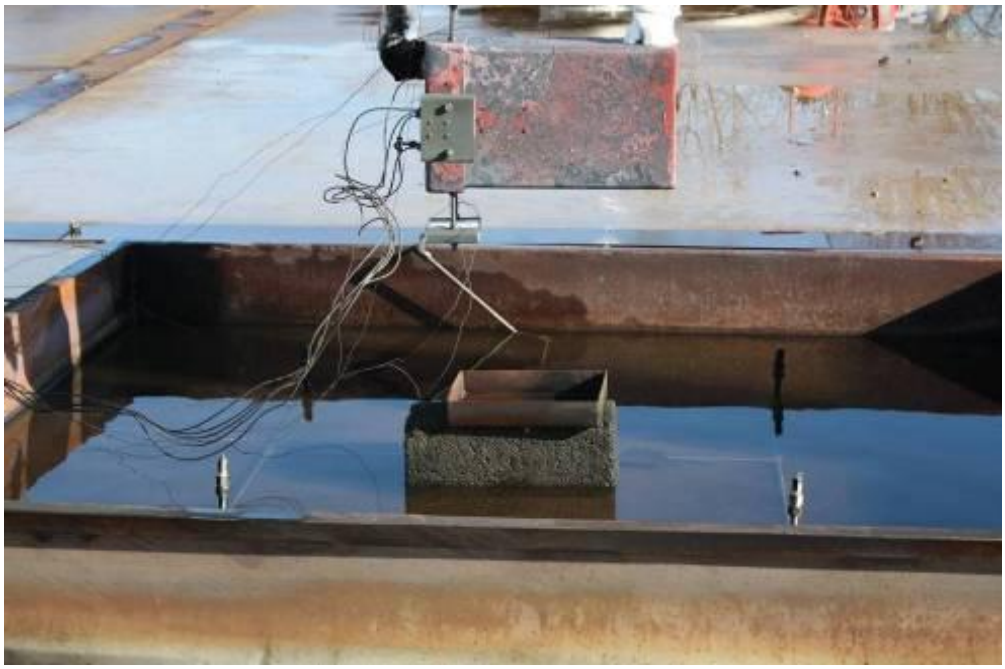

(b) Photograph of heptane spray manifold just prior to testing.

Figure 37. Heptane spray fire system.

5.1.2 Propane Area Burner

A propane area burner comprised of 16 multi-orifice spray heads fed by an interconnected piping system was designed and constructed. The footprint of the area burner was ~1.0 m (3.3 ft) square. The spray heads were installed in a 4 × 4 array and spaced 0.3 m (12 in) on center. Each spray head was comprised of 19 4.8-mm (0.1875-in) holes that are uniformly distributed over the top of the spray head. For this testing, the exterior ring of holes, 12 in total, was plugged such that exiting propane was discharged through the remaining 7 holes, with a total discharge orifice area of 125 mm^2 (0.19 in^2). Propane was supplied to each spray head from the bottom through a 19-mm (0.75-in) NPT pipe network. The propane supply was provided by a 227-kg (500-lb) horizontal propane tank, with a nominal diameter of 1.1 m (44 in) and a length of 2.6 m (104 in). A 19-mm (0.75-in) liquid supply port was provided with the tank such that liquid propane could be delivered to a vaporizer. Approximately 6.1 m (20 ft) of 19-mm (0.75-in) piping was used to connect the propane tank and vaporizer. The vaporizer used in this testing was an Alternative Energies Model AE-40 vaporizer, with a listed vaporization capacity of 4.2×10^{-5} m^3/s (40 gph). A photograph of the spray heads is provided in figure 38.

Figure 38. Photograph of spray heads to be used in propane area burner.

The piping network used to supply the spray heads was a gridded system that was supplied from four different locations to ensure uniform gas distribution. An illustration of this supply network is shown in figure 39a. The majority of the system piping was constructed from 25.4-mm (1-in) steel piping. Bell reducers were used to transition from the 25.4-mm (1-in) network up to the 19-mm (0.75-in) pipe stems on which the spray heads are mounted. Both a schematic and photograph of the propane area burner system are provided in figure 39. The pipe stems on which the spray heads will be installed elevated the heads ~0.2 m (8 in) above the concrete pad in order to establish adequate entrainment into the propane area fire. The piping network was made to be modular using 25.4-mm (1-in) unions connecting each f4-head branch line. This modular design could be used to easily modify the burner for larger objects, if needed. For this test series, the propane area burner was centered within the 2.2-m (7.1-ft) square fuel pan used in

the STANAG 4240 fire tests previously conducted at NRL/CBD. A photograph of the propane area fire test apparatus is shown in figure 39. As shown in figure 39, during testing, the fuel pan was filled with water to mitigate heating/warping of the pan as well as to enhance the propane flow through added heat exchange with the piping environment.

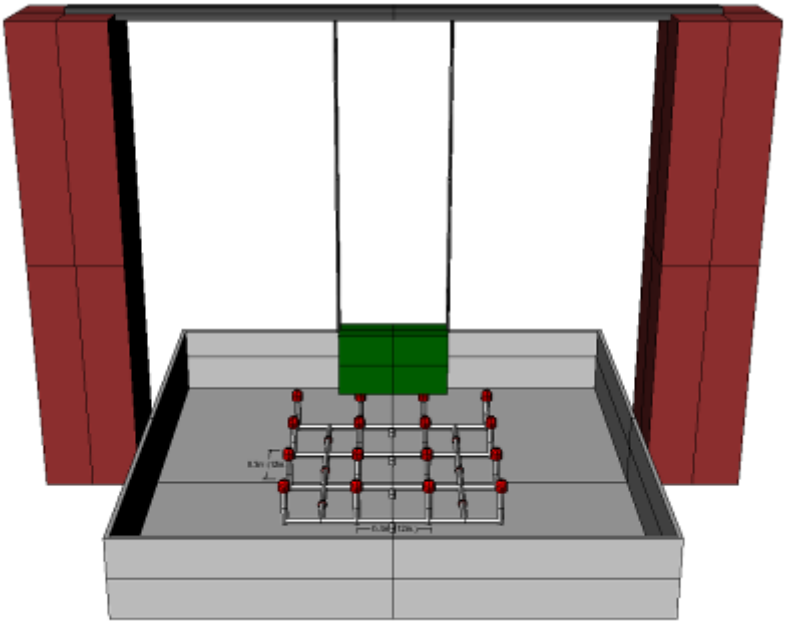

(a) Rendering of propane area burner

(b) Photograph of propane area burner just prior to testing

Figure 39. Propane area burner.

Initially, the flow of propane to the burner was to be measured using a pair of Dwyer Model RMC rotameters with a total flow capacity of 0.03 m^3/s (3600 scfh). The flow meters were installed downstream of the vaporizer with both pressure and temperature measurements in line. However, this method of measurement was only used during the first couple of minutes of the first propane fire exposure due to the fact that liquid propane was being transported through the lines and into the rotameters. After this, the rotameters were removed and replaced with piping. Consequently, the exact fire sizes associated with these exposures are not known. However, these fire sizes were approximated using the data collected during the first couple of minutes of the test as well as using empirical correlations. A discussion of the data analysis and correlations used is presented in section 5.1.4.

5.1.3 Propane Jet Burners

The second propane system evaluated consisted of a pair of jet burners comprised of eight horizontally oriented 19.1-mm (0.75-in) open pipe ends. The burner was comprised of two parallel lines of spray nozzles directed into the center of the 2.2-m (7.1-ft) square fuel pan (i.e., towards the suspended instrumented container), as shown in figure 40.

Figure 40. Photograph of propane spray burner system.

The piping system consisted of a 25.4-mm (1-in) diameter steel pipe that was reduced down to a 19.1-mm (0.75-in) orifice at the discharge end. Four of these pipes were plumbed in parallel and fed from a single, centrally located inlet (as shown in figure 40). The pipes were laterally offset 0.25 m (10 in) from one another. This spacing was selected such that the span of the spray burner is greater than the longest dimensions of the instrumented box. The discharging orifice of the burners was installed 0.2 m (8 in) above the lip of the fuel pan, thus locating them ~0.15 m

(6 in) below the base of the instrumented box. The nozzles were offset from the vertical walls of the instrumented box at a distance of 0.53 m (21 in). The vertical and horizontal offsets adopted for this test were selected such that the turning region of the flame jets emitted by the burners (i.e., the point at which the jets transition from horizontal to vertical travel) occurs just prior to or just beneath the suspended container, thus immersing the box in flame. During testing, the fuel pan was filled with a 50.4-mm (2-in) layer of water to mitigate heating/warping of the pan.

5.1.4 Propane Fire Size Approximations

As previously mentioned, propane flow rates were only briefly measured during the first propane fire exposure and could not be completely measured in either propane fire exposure due to the inability of the propane vaporizer to adequately vaporize the quantity of propane required for these tests. This inability resulted in liquid propane being transported into the piping system, producing a two-phase flow scenario and an unknown quantity of gaseous propane being discharged from the aforementioned burners. The transport of liquid propane did not occur until ~1–2 min after initiating gas flow in the first test. Consequently, it is known that a nominal flow rate of 0.024 m^3/s (3000 scfh) was being discharged during this phase of the test producing an approximate 1.6 MW fire. Although the propane flow rate could not be measured directly for the duration of these tests, the aforementioned value does provide some indication of the nominal size of the fire. Further, verification of this fire size was accomplished using the observed flame height and equivalent burner diameter for the propane spray burner fire in conjunction with the flame height correlation developed by Heskestad to approximate the fire size. The correlation used to approximate fire size is presented in equation 15.

$$L_f = 0.235Q^{2/5} - 1.02D \ , \tag{15}$$

where L_f is the pool fire flame height (m), Q is the pool fire heat release rate (kW), and D is the pool fire diameter (m).

5.2 Alternative Fuel Fire Exposure Results and Analysis

Four alternative fuel fire exposure tests were conducted—two using heptane and two using propane. The heptane spray fire was conducted in duplicate, while each of the propane fires were unique and only conducted once. In general, the fire exposures created by these alternative fuel fires were comparable to those generated in the STANAG pool fires as measured by the instrumented box and were conducted under generally similar conditions. A summary of the fire exposure durations, fire conditions, and average ambient conditions during these exposures is provided in table 12.

Table 12. Summary of test conditions for alternative fuel fire exposures.

Test Case	Flame Duration (min)	Ambient Temperature (°C [°F])	Average Wind Speed (kph [mph])	Time After Ignition That Temperature at Two Locations Is >550 °C (1022 °F) [s]	Time After Ignition That Mean Temperature at All Locations Reaches 800 °C (1472 °F) [s]	Average Flame Temperature (°C [°F])
Heptane	14	5 [41]	2.2 [1.3]	9	4	929 [1705]
Spray	11.5	5 [41]	1.8 [1.1]	5	9	882 [1619]
Propane area	11.8	6 [43]	3.2 [2.0]	11	185	721 [1347]
Propane line	13.5	6 [43]	3.6 [2.2]	15	148	673 [1244]

5.2.1 Heptane Spray Burner – Test 1

The first heptane spray fire test was conducted in a manner similar to that used in the aforementioned STANAG 4240 pool fire tests. In this test, the fuel collection pan was filled with ~50.8 mm (2 in) of water, and the spray nozzles were installed 50.8 mm (2 in) above the water surface. The instrumented box was elevated 0.51 m (20 in) above the spray nozzles. This elevation differs from that used in the STANAG 4240 tests, where a box elevation of 0.36 m (14 in) was used. In this test, the box was elevated an additional 0.15 m (6 in) to ensure immersion in the fire plume given the expected spray pattern of the nozzles. Had the box been elevated only 0.36-m (14-in) above the nozzles, it is likely that some portion of the box would have been below the fire plume, thus providing erroneous fire exposure data. Once the instrumented box and heptane spray fire test apparatus were installed, a 0.3-m (12-in) square pilot pan was installed at the center of the spray rig. The pan was installed atop a concrete block, thus elevating the pan 0.2-m (8-in) above the base of the fuel collection pan. This pan served as the ignition source for this fire exposure.

Two minutes of data was collected prior to the ignition of the heptane spray fire. After background data collection was initiated, video cameras were activated, and fuel was poured into the pilot pan. The pan was filled with ~0.25 L (0.07 gal) of gasoline and lit just prior to initiating flow to the spray nozzles. Once ignited, the flow rate of heptane was monitored and recorded using the pressure transducer installed in the fuel supply tank. In this test, the average measured tank pressure was 47 psi which, based upon the k-factor of the spray nozzles resulted in a nominal heptane flow rate of 1.2 gpm per nozzle with a total flow rate of 4.7 gpm. In this test, the average wind speed over the duration of the exposure was 2.2 kph (1.3 mph). A photograph of the fire exposure generated in the first heptane spray fire test is provided in figure 41.

Figure 41. Representative photograph of fire exposure generated during the first heptane spray fire.

In general, the operation of the heptane spray fire was found to be easily managed and reliable. Once the fuel tank was filled and pressurized, the exposure fire was controlled via the operation of a single valve. Adjustments in fire size were performed manually through changes in fuel tank pressure. The conical spray pattern produced by the spray nozzle rig enveloped the instrumented box resulting in complete immersion of the container in fire. As shown in figure 41 and during the majority of this test, the heptane spray fire produced an optically thick flame plume (i.e., the flame envelopment was such that the box was not visible). Furthermore, the immediate ignition and atomization of the fuel spray by the nozzles was such that a very small quantity of fuel was not consumed during the exposure. In general, fuel not consumed by the exposure fire was readily evaporated when it came into contact with neighboring hot surfaces (i.e., fuel pan, concrete deck, etc.).

In this test, an average flame temperature of 550 °C (1022 °F) was reached 9 s after ignition. Per the requirements of STANAG 4240, this time will be denoted as time zero for this test in all future discussions. The 800 °C (1472 °F) threshold specified in STANAG 4240 was achieved in 4 s after time zero. As a result of the spray fire being manually secured, the average flame temperature dropped below 550 °C (1022 °F) 841 s after time zero. This will be considered as the end of the exposure for all calculations. The average flame temperature measured during this test was 929 °C (1705 °F). A summary of the various calculated heat fluxes measured during this test is presented in table 13. Average flame temperatures, calculated wall heat fluxes, and calculated plate heat fluxes measured in this test are presented in figure 42.

Table 13. Summary of heat flux data collected during the first heptane spray fire test.

Measurement Type	**Measurement Location**	**Avg. Heat Flux (kW/m^2)**	**Peak Heat Flux (kW/m^2)**
Wall	1	143	160
	2	96	140
	3	85	140
	4	109	140
	5	111	140
Plate	1	148	175
	2	60	112
	3	78	123
	4	100	130
Exposure to Walls		**109**	**160**
Exposure to Plates		**97**	**175**

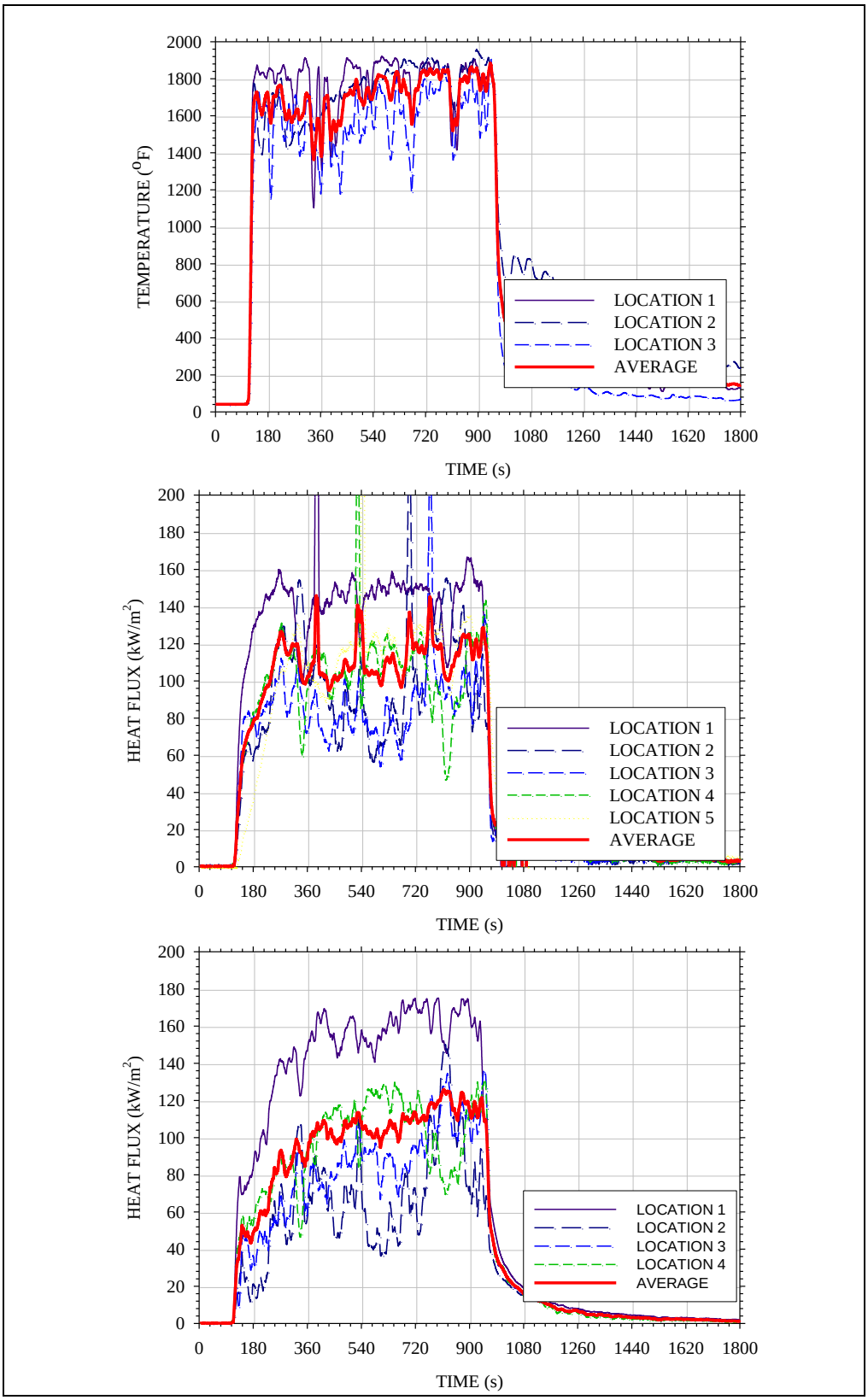

Figure 42. Plot of temperatures (top), calculated wall heat flux (bottom left), and calculated plate heat flux (bottom right) measured in the first heptane spray fire test.

As shown in table 13, the calculated heat fluxes on the vertical faces of the container (i.e., the faces of the container that were perpendicular to the fuel surface) were consistently higher than those measured on surfaces parallel to the fuel surface (i.e., topside and fire side). On average, the vertical face heat fluxes were 11 kW/m^2 greater than those measured on horizontal surfaces when using the wall heat fluxes and 33 kW/m^2 greater when using plate surfaces. The average heat flux exposure to the instrumented container in this test was 109 kW/m^2 as measured on the walls and 97 kW/m^2 as measured on the plate thermometers.

5.2.2 Heptane Spray Burner – Test 2

The second heptane spray fire test was conducted using the same test procedures as described in section 5.2.1. In this test, the average measured tank pressure was 46 psi which, based upon the k-factor of the spray nozzles, resulted in a nominal heptane flow rate of 1.2 gpm per nozzle with a total flow rate of 4.7 gpm. In this test, the average wind speed over the duration of the exposure was 1.8 kph (1.1 mph). A photograph of the fire exposure generated in the first heptane spray fire test is provided in figure 43.

The fire exposure generated during the second heptane spray fire was comparable to that observed in the first heptane test. The flame plume was generally optically thick enough such that the box was not visible when immersed. It should also be noted from figure 43 that the smoke plume generated in this test is substantially less than that produced by the liquid fuel pool fires described in the previous section (see figure 31 for comparison).

In this test, an average flame temperature of 550 °C (1022 °F) was reached 5 s after ignition. Per the requirements of STANAG 4240, this time will be denoted as time zero for this test in all future discussions. The 800 °C (1472 °F) threshold specified in STANAG 4240 was achieved in 9 s after time zero. The average flame temperature dropped below 550 °C (1022 °F) 687 s after time zero. This will be considered as the end of the exposure for all calculations. The average flame temperature measured during this test was 882 °C (1619 °F). A summary of the various calculated heat fluxes measured during this test is presented in table 14. Average flame temperatures, calculated wall heat fluxes, and calculated plate heat fluxes measured in this test are presented in figure 44.

As shown in table 14, the calculated heat fluxes on the vertical faces of the container (i.e., the faces of the container there were perpendicular to the fuel surface) were consistently higher than those measured on surfaces parallel to the fuel surface (i.e., topside and fire side). On average, the vertical face heat fluxes were 11 kW/m^2 greater than those measured on horizontal surfaces when using the wall heat fluxes and 27 kW/m^2 greater when using plate surfaces. The average heat flux exposure to the instrumented container in this test was 99 kW/m^2, as measured on the walls and 90 kW/m^2 as measured on the plate thermometers.

Figure 43. Photograph of second heptane spray fire exposure.

Table 14. Summary of heat flux data collected during the second heptane spray fire test.

Measurement Type	**Measurement Location**	**Avg. Heat Flux (kW/m^2)**	**Peak Heat Flux (kW/m^2)**
Wall	1	106	153
	2	112	140
	3	96	140
	4	74	112
	5	109	140
Plate	1	117	148
	2	93	170
	3	89	126
	4	60	92
Exposure to Walls		**99**	**153**
Exposure to Plates		**90**	**170**

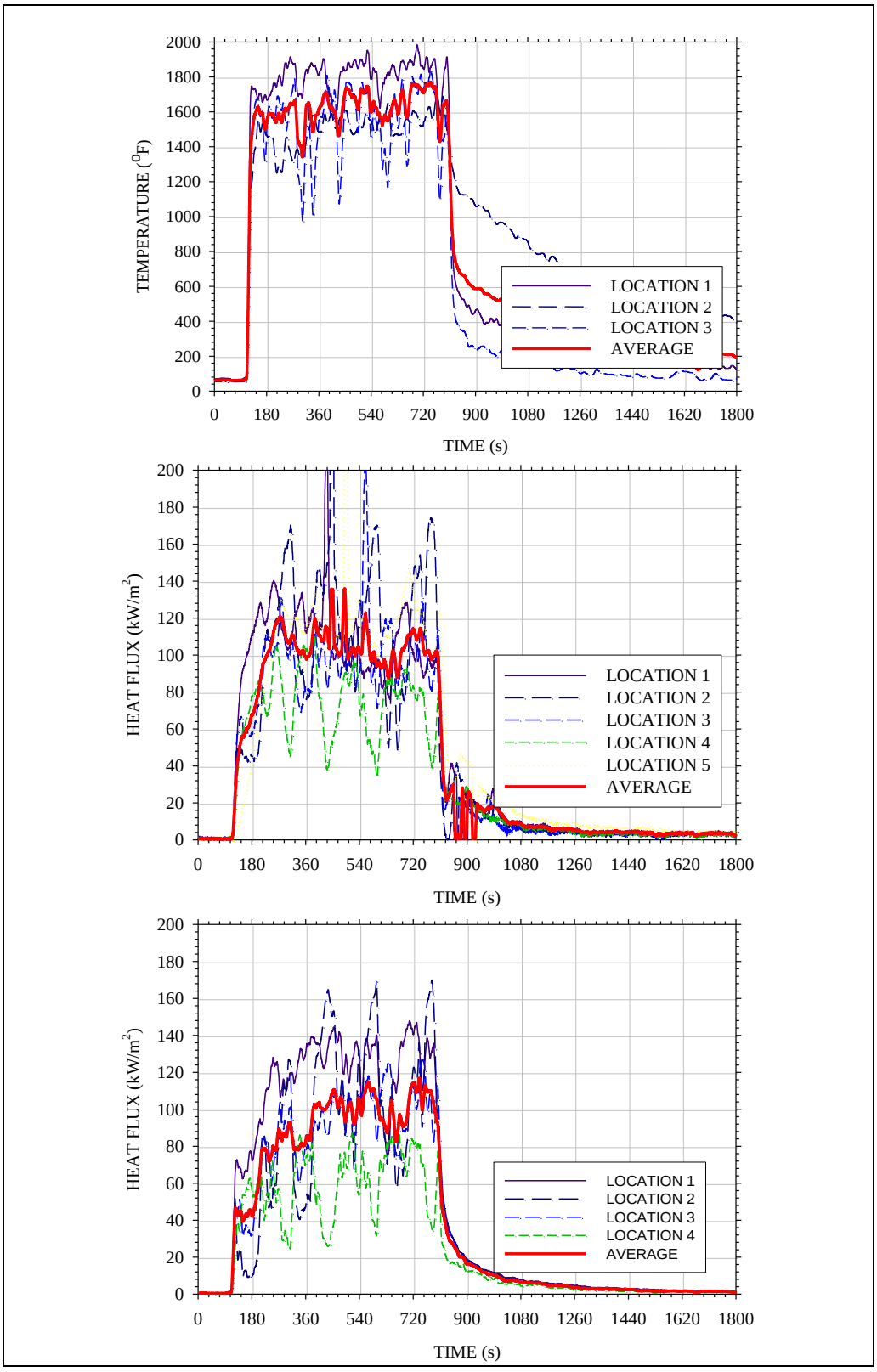

Figure 44. Plot of temperatures (top), calculated wall heat flux (bottom left), and calculated plate heat flux (bottom right) measured in the second heptane spray fire test.

5.2.3 Propane Area Burner

The propane area fire test was conducted in a manner similar to that used in the aforementioned STANAG 4240 pool fire tests. The elevation of the instrumented box above the burner nozzles was consistent with that used in the STANAG 4240 testing (i.e., 0.36 m [14 in]). Two minutes of data was collected prior to the ignition of the propane fire. After background data collection was initiated, video cameras were activated, and fuel was poured into the pilot pan. For this test, the pilot pan was positioned in the center of the propane area burner. The pan was filled with ~0.25 L (0.07 gal) of gasoline and lit just prior to initiating flow to the spray nozzles. Once ignited, the flow rate of propane was governed by the rate of heat transfer into the LPG tank. In this test, the average wind speed over the duration of the exposure was 3.2 kph (2.0 mph). A photograph of the fire exposure generated in the first heptane spray fire test is provided in figure 45.

Figure 45. Photograph of propane area fire.

Unlike that reported for the heptane spray burner, the operation and control of the propane area fire was slightly more challenging due to the need for additional equipment and instrumentation. As mentioned earlier, the propane fire exposures required that liquid propane be transported to a vaporizer and then that the resulting gaseous propane flow rate be measured and transported to the burner. This process proved troublesome in that the vaporizer did not provide sufficient heating; thus, liquid propane was being transported through the gaseous propane piping, thus hindering the ability to measure flow rates.

In this test, an average flame temperature of 550 °C (1022 °F) was reached 11 s after ignition. Per the requirements of STANAG 4240, this time will be denoted as time zero for this test in all future discussions. The 800 °C (1472 °F) threshold specified in STANAG 4240 was achieved in 185 s after time zero. The average flame temperature dropped below 550 °C (1022 °F) 709 s after time zero. This will be considered as the end of the exposure for all calculations. The average flame temperature measured during this test was 731 °C (1347 °F). A summary of the various calculated heat fluxes measured during this test is presented in table 15. Average flame temperatures, calculated wall heat fluxes, and calculated plate heat fluxes measured in this test are presented in figure 46.

Table 15. Summary of heat flux data collected during the propane area fire test.

Measurement Type	**Measurement Location**	**Avg. Heat Flux (kW/m^2)**	**Peak Heat Flux (kW/m^2)**
Wall	1	48	91
	2	36	74
	3	82	140
	4	76	140
	5	86	140
Plate	1	30	70
	2	18	54
	3	66	91
	4	70	80
Exposure to Walls		**65**	**140**
Exposure to Plates		**46**	**91**

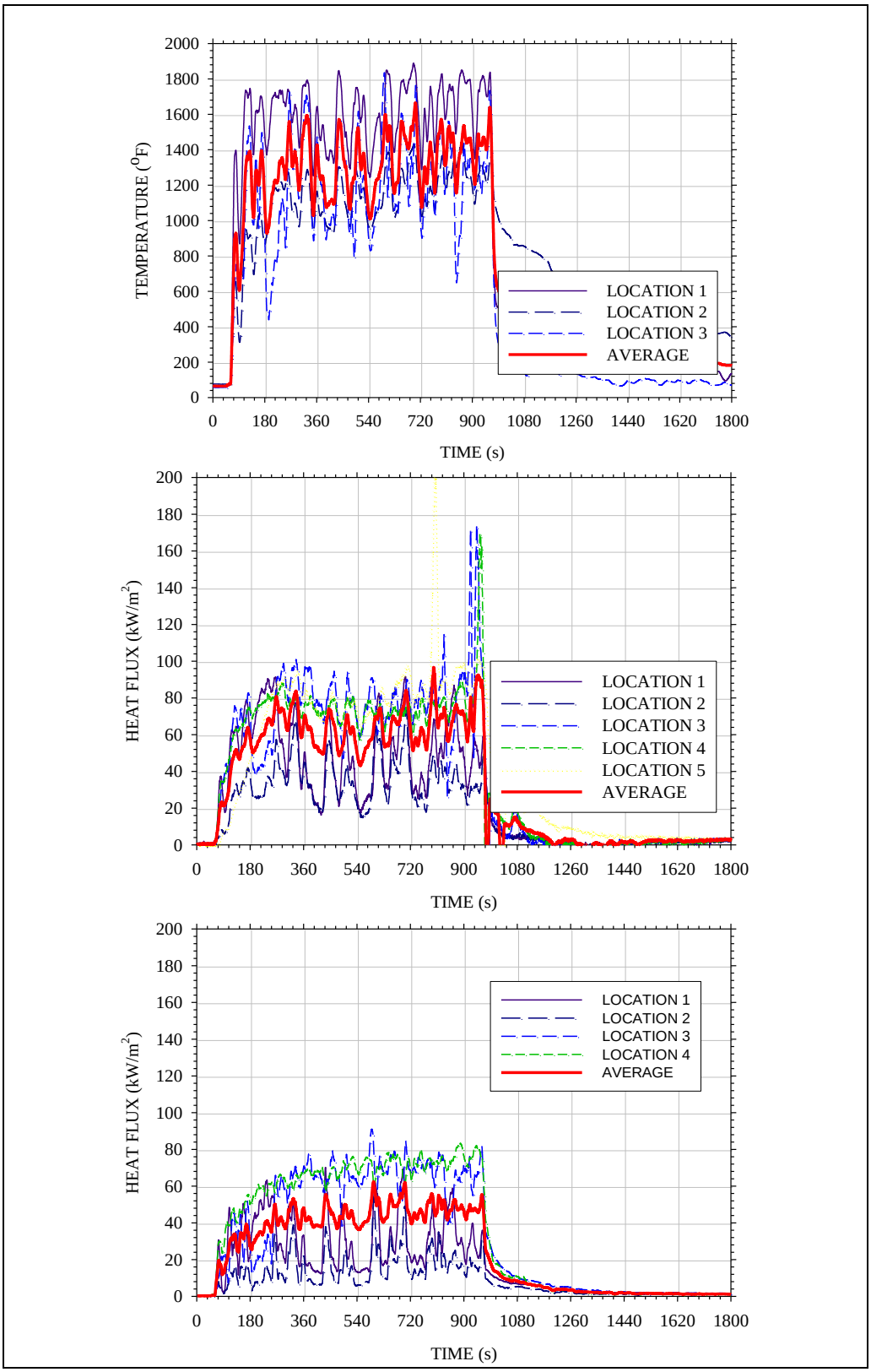

Figure 46. Plot of temperatures (top), calculated wall heat flux (bottom left), and calculated plate heat flux (bottom right) measured in the propane area fire test.

As shown in table 15, the calculated heat fluxes on the vertical faces of the container (i.e., the faces of the container that were perpendicular to the fuel surface) were consistently higher than those measured on surfaces parallel to the fuel surface (i.e., topside and fire side). On average, the vertical face heat fluxes were 16 kW/m^2 greater than those measured on horizontal surfaces when using the wall heat fluxes and 4 kW/m^2 greater when using plate surfaces. The average heat flux exposure to the instrumented container in this test was 65 kW/m^2 as measured on the walls and 46 kW/m^2 as measured on the plate thermometers. In this test, an average flame height of 3.5 m (11.3 ft) was observed. Using these data, coupled with the equivalent diameter of the propane spray burner being 1.13 m (3.7 ft) and the correlation presented in equation 11, an approximate fire size of 1.7 MW was calculated. This value is similar to that calculated based upon the brief measurement of propane flow rate collected in the early stages of this test (1.6 MW).

5.2.4 Propane Jet Burner

The propane jet fire test was conducted using the same test procedures as described in section 5.2.2. The elevation of the instrumented box above the burner nozzles was consistent with that used in the STANAG 4240 testing (i.e., 0.36 m [14 in]). Two minutes of data were collected prior to the ignition of the propane fire. After background data collection was initiated, video cameras were activated, and fuel was poured into the pilot pan. For this test, the pilot pan was positioned in the center of the fuel collection pan. The pan was filled with ~0.25 L (0.07 gal) of gasoline and lit just prior to initiating flow to the spray nozzles. Once ignited, the flow rate of propane was monitored and recorded using the pressure transducer installed in the fuel supply tank. In this test, the average measured tank pressure was 47 psi which, based upon the k-factor of the spray nozzles, resulted in a nominal heptane flow rate of 1.2 gpm per nozzle with a total flow rate of 4.7 gpm. In this test, the average wind speed over the duration of the exposure was 3.6 kph (2.2 mph). A photograph of the fire exposure generated in the propane spray fire test is provided in figure 47.

In this test, an average flame temperature of 550 °C (1022 °F) was reached 15 s after ignition. Per the requirements of STANAG 4240, this time will be denoted as time zero for this test in all future discussions. The 800 °C (1472 °F) threshold specified in STANAG 4240 was achieved in 148 s after time zero. The average flame temperature dropped below 550 °C (1022 °F) 809 s after time zero. This will be considered as the end of the exposure for all calculations. The average flame temperature measured during this test was 673 °C (1244 °F). A summary of the various calculated heat fluxes measured during this test is presented in table 16. Average flame temperatures, calculated wall heat fluxes, and calculated plate heat fluxes measured in this test are presented in figure 48.

Figure 47. Photograph of propane jet burner.

Table 16. Summary of heat flux data collected during the propane spray fire test.

Measurement Type	**Measurement Location**	**Avg. Heat Flux (kW/m^2)**	**Peak Heat Flux (kW/m^2)**
Wall	1	41	92
	2	38	86
	3	58	94
	4	52	61
	5	63	75
Plate	1	24	65
	2	22	64
	3	44	80
	4	43	55
Exposure to Walls		**51**	**94**
Exposure to Plates		**33**	**94**

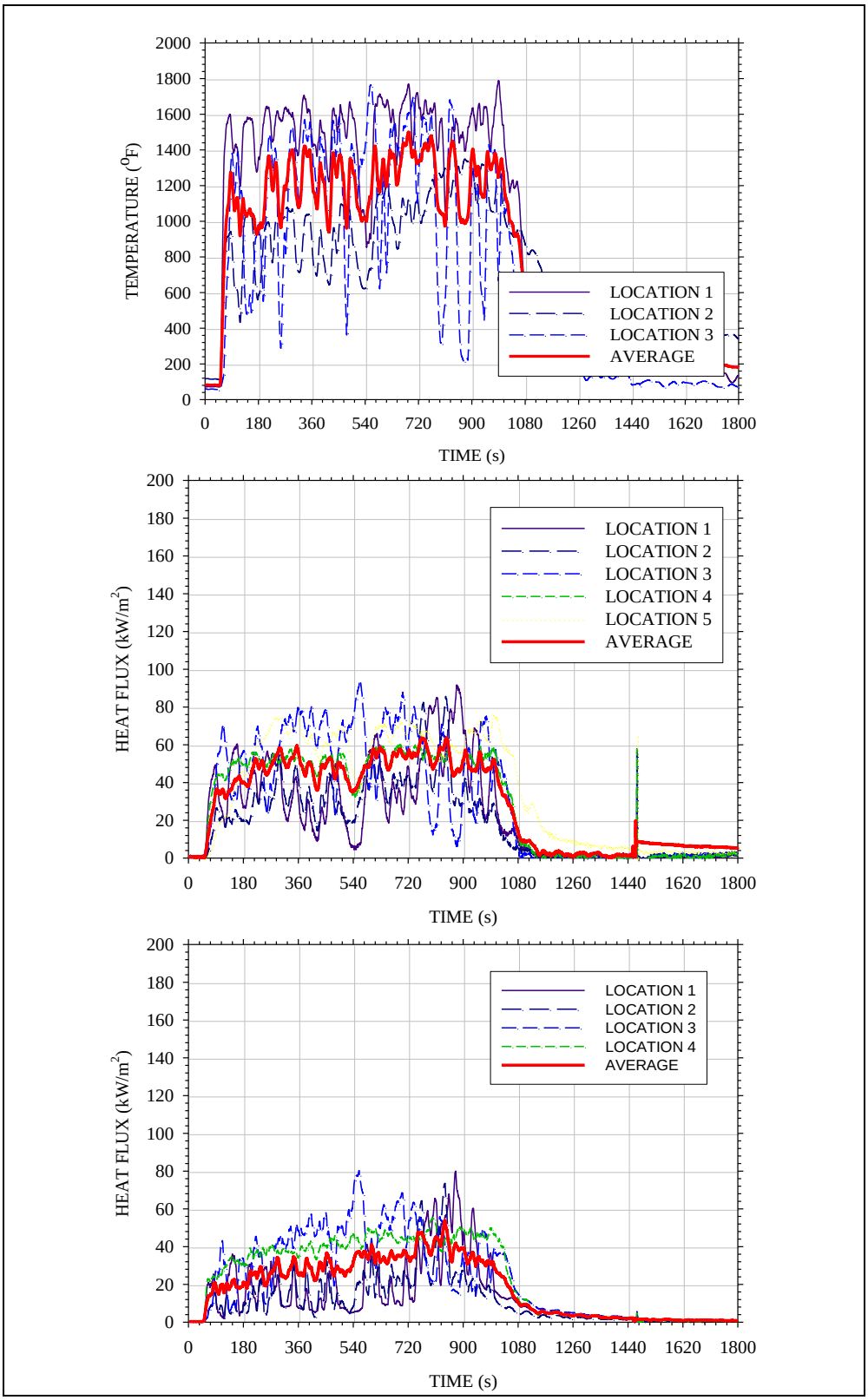

Figure 48. Plot of temperatures (top), calculated wall heat flux (bottom left), and calculated plate heat flux (bottom right) measured in the propane spray fire test.

As shown in table 16, the calculated heat fluxes on the vertical faces of the container (i.e., the faces of the container that were perpendicular to the fuel surface) were consistently higher than those measured on surfaces parallel to the fuel surface (i.e., topside and fire side). On average, the vertical face heat fluxes were 9 kW/m^2 and greater than those measured on horizontal surfaces when using the wall heat fluxes and 2 kW/m^2 greater when using plate surfaces. The average heat flux exposure to the instrumented container in this test was 51 kW/m^2 as measured on the walls and 33 kW/m^2 as measured on the plate thermometers. Given that the flow settings used in this test were the same as those used in the previous propane exposure fire and the total orifice sizes from both burners were nominally the same, it is assumed that the fire size produced in the propane jet burner is comparable to that obtained in the propane area burner (i.e., ~1.2–1.7 MW).

5.3 Comparison of Alternative Fuel Fires to STANAG 4240 Exposure

Three different alternative fuel fire exposures were considered—a heptane spray fire exposure, a propane area burner, and a propane line burner. The data collected from these exposures have been summarized and compared to measured STANAG 4240 pool fire exposure data in table 17 and plotted in figures 49–51.

Table 17. Summary of heat flux exposure data measured during STANAG 4240 testing.

Measurement Location	**Average Measured Heat Flux (kW/m^2)**			
	STANAG Pool Fire	**Heptane Spray Fire**	**Propane Area Fire**	**Propane Line Fire**
Wall	84 ± 7	104 ± 5	65	51
Plate	72 ± 10	94 ± 4	46	33
Measurement Location	**Measured Peak Heat Flux (kW/m^2)**			
	STANAG Pool Fire	**Heptane Spray Fire**	**Propane Area Fire**	**Propane Line Fire**
Wall	135 ± 6	157 ± 4	140	94
Plate	135 ± 5	173 ± 3	91	94

As shown in both table 17 and figures 49–51, the heptane spray fire produced the most severe thermal exposure to the instrumented box. The average and peak values measured at all locations during this alternative fuel fire exposure were greater than measurements taken at the same locations during all other exposures. The STANAG 4240 pool fire exposure resulted in the next most severe exposure with both propane exposures producing the least thermally severe conditions.

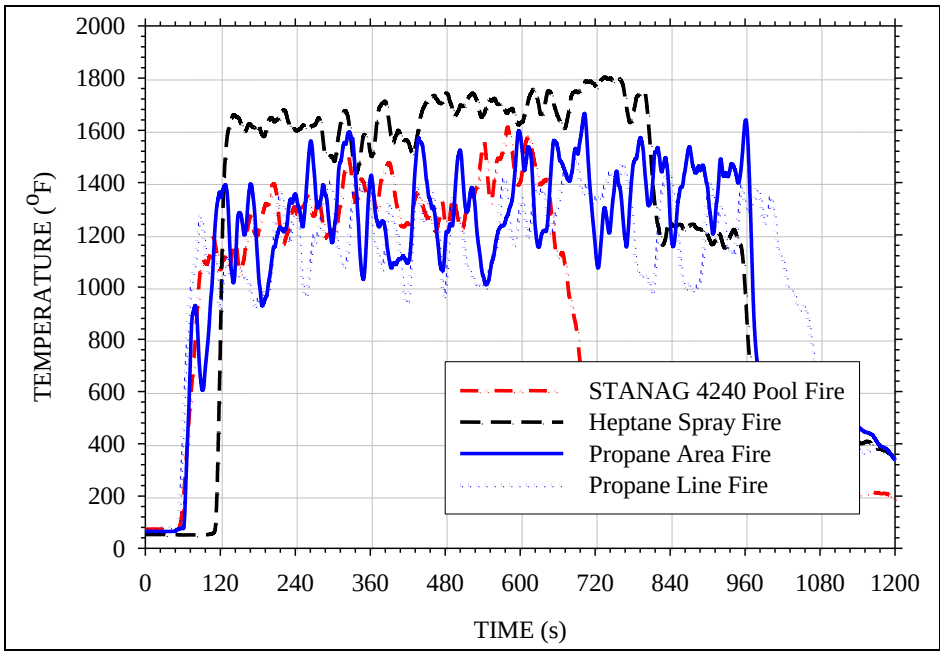

Figure 49. Comparison of fire temperatures from both STANAG 4240 pool fire exposure and alternative fuel fire exposures.

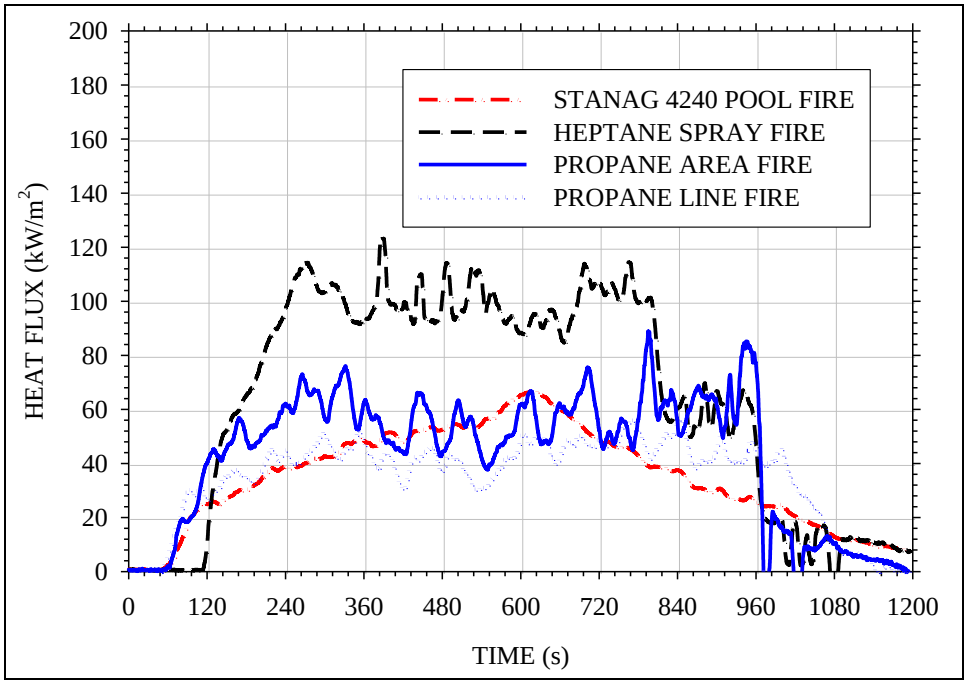

Figure 50. Comparison of wall heat flux measurements from both STANAG 4240 pool fire exposure and alternative fuel fire exposures.

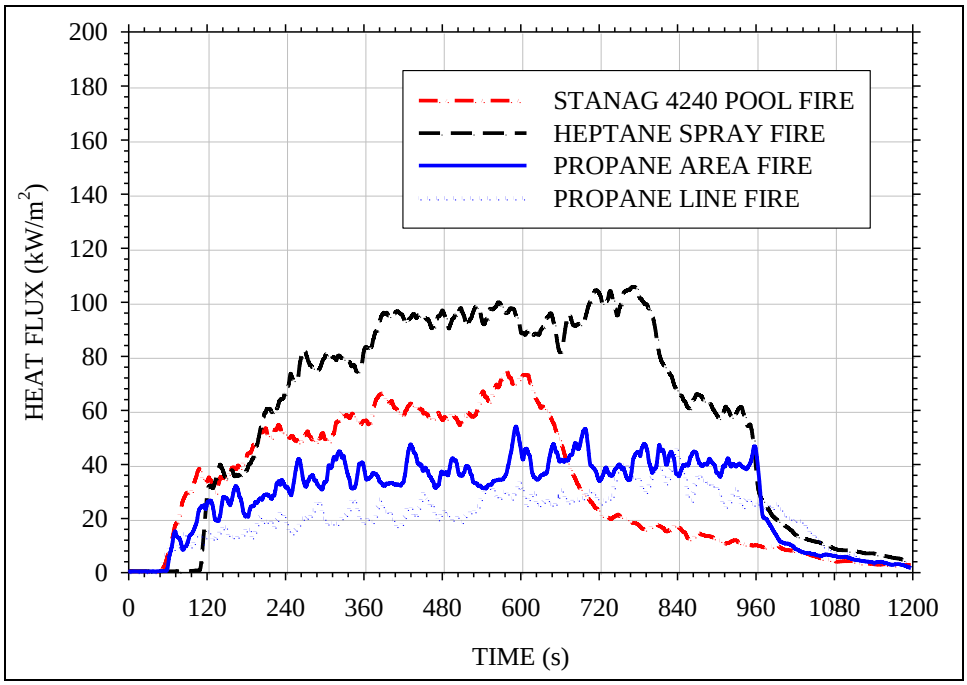

Figure 51. Comparison of wall heat flux measurements from both STANAG 4240 pool fire exposure and alternative fuel fire exposures.

6. Phase V – Comparison of Alternatives Fuel Exposures

The identification of a viable fire exposure alternative to the current STANAG 4240 pool fire cannot be made solely on thermal exposure characteristics; it must also include consideration of both the environmental and operational cost-benefit of the system. A viable alternative should not only provide an equivalent thermal exposure with less environmental impact but should also improve the level of control over the fire exposure. As discussed earlier, the current STANAG 4240 liquid fuel fire exposure uses a large amount of liquid fuel, provides little operator control, and has a significant impact on the environment each time a test is conducted. The level of control over the fire exposure is minimal given that once the liquid fuel is ignited, it must burn to completion. The purpose of this section is to describe the costs and benefits associated with the implementation of these alternative fire exposures at various scales. These costs/benefits will be assessed in terms of material, operations, and environmental impacts. In order to make direct comparisons between the current pool and the alternative fuel fires proposed in this work, it is necessary to establish some sense of scaling the alternative fuel fire exposures.

Based upon the work conducted in this study, it was concluded that both alternative fuel fire exposures considered (i.e., heptane and propane) were capable of producing thermal exposures comparable to that produced by the STANAG 4240 pool fire. Using this conclusion, a nominal

burner configuration per unit area was developed. For the heptane spray fire exposure, it was determined that a single Bete P-80 spray nozzle flowing at a rate of 0.06 L/s (1 gpm) was sufficient to cover an area of 1 m^2 (10.8 ft^2). Generating a comparable exposure using the propane nozzles tested in this work required that a total of four nozzles be installed per square meter of exposure. These four nozzles were flowing at a rate of 0.018 L/s (0.29 gpm). These configurations per unit area will be used to make comparisons between the operational costs of the STANAG 4240 and alternative fuel fire exposures.

6.1 Cost of Operation

In the STANAG 4240 exposure fires conducted in this work, a total of 208 L (55 gal) of JP-5 fuel was used per test. Once ignited, the fuel burned for 12 min on average. Over the same time frame, the heptane spray burner considered in this work would have used ~87% of that, consuming a total of 181 L (48 gal) of heptane. The propane fire exposures, if conducted over the same time frame, would use ~41% of the fuel required for the STANAG 4240 exposure, consuming a total of 87 L (23 gal) of propane.

The first example case is based upon the testing of a RAN 5 in/54 cartridge case (*19*). A photograph of the test is provided in figure 52. As shown in the figure, the cartridge case was suspended above a 9-m (30-ft) square pool of fuel, lined with a plastic, waterproof lining. The pool was filled with 4800 L (1268 gal) of aviation fuel. The fire exposure in this test burned for ~9 min with an average regression rate of 6.6 mm/min (0.24 in/min). Using the same alternative fuel spray nozzle configurations used in the aforementioned mini-fuel fire exposures (i.e., one nozzle per square meter for the heptane exposure and four nozzles per square meter for the propane configuration), fuel consumption values were calculated.

Figure 52. Photograph of STANAG 4240 test setup evaluating the response of a RAN 5 in/54 cartridge case (*19*).

Per the configuration description just provided, 81 spray nozzles would be required to provide a thermal exposure comparable to the 81 m^2 (872 ft^2) pool fire. These nozzles would discharge a total of 2760 L (729 gal) of heptane over a 9-min test duration, which is ~57% of that used in the STANAG pool fire. Similarly, the propane exposure fire would require a total of 324 propane nozzles to produce an exposure comparable to that produced in the STANAG 4240 pool fire. This configuration would consume a total of 778 L (205 gal) of propane, which is ~16% of that consumed in the pool fire exposure.

The second example case considered is not based upon a specific test conducted but instead represents a bounding scenario in which the exposure fire size is very large. For this scenario, a 30-m (98-ft) square pool fire is considered. A standard STANAG 4240 pool fire exposure for this size fire would require that 53,100 L (14,030 gal) of fuel be provided. This quantity of fuel would provide a fuel layer that is nominally 59-mm (2.3-in) thick, which, if a regression rate of 6.6 mm/min is assumed, would result in exposure duration of ~9 min. Using this fire size and exposure duration the heptane spray fire previously discussed would require a total of 900 nozzles and would consume a total of 30, 661 L (8100 gal) of heptane while the propane system would require 3600 nozzles consuming 864 L (2230 gal). The percent fuel savings for the both the heptane and propane fuels in this case were similar to those identified in the first example case, 40% and 80% savings, respectively.

A summary of the volume of fuel consumed in each of the three aforementioned exposure fire scenarios for each fuel type is provided in table 18. Also provided in table 18 is an estimate of the cost savings provided by the alternative fuels when compared to the current fuels specified in STANAG 4240. These cost savings are based upon per gallon fuel costs of $2.94, $5.45, and $3.00 for JP-5, heptane, and propane (liquid), respectively.

As shown in table 18, while from a quantity consumed standpoint, the heptane spray fire exposure provides substantial savings; due to the increased cost of the fuel, the cost savings are negated. However, this is not the case for the propane exposure fires, which show substantial fuel and fuel cost savings when compared to the standard STANAG 4240 liquid pool fire exposure. Given that the cost of the propane and STANAG 4240 liquid fuels are equivalent, the fuel cost savings associated with the use of propane are comparable to fuel quantity savings (i.e., 58%–84%).

It should be noted that the cost savings just presented are strictly based upon fuel costs and do not take into the account the increased facilities and operational costs associated with the storage, transport, and vaporization of large quantities of propane. While these costs are expected to be significant, it is also expected that the bulk of the expense will be a one-time cost for the installation/commissioning of the facility and once commissioned the operating costs should not be such that the savings provided by the use of the propane is negated.

Table 18. Comparison of operational cost benefits provided by alternative fuel fire exposures.

Scenario	Exposure Area (fr2)	Exposure Duration (min)	Volume of Fuel Require (gal)			Fraction of Fuel Saved Using Alternative Fuel			Total Fuel Cost		
			STANAG[a]	Heptane	Propane	STANAG	Heptane	Propane	STANAG[b]	Heptane[b]	Propane[b]
Mini-fuel fires	52	9	55	48	23	—	0.13	0.58	$161.70	$261.60	$69.00
Example 1 – RAN 5/54	872	9	1268	729	205	—	0.43	0.84	$3,727.92	$3,973.05	$615.00
Example 2 – Bounding scenario	9688	9	14030	8100	2283	—	0.42	0.84	$ 41,248.20	$ 44,145.00	$ 6,849.00

[a]Assuming nominal fuel depth of 51–76 mm (2–3 in).
[b]Fuel cost savings calculated using unit cost data provided.

6.2 Exposure Control and Repeatability

The current STANAG 4240 pool fire exposure provides very little control and assurance of test repeatability to the operator given the type of fuel used and the scale of fire typically conducted. Other than the test operator's ability to control when the fire exposure begins, there is no other form of control available when conducting the large-scale pool fire. This is not true when considering either the heptane or propane fire exposures developed in this work. In both cases, the exposure fire size and duration can be controlled by the test operator remotely. The flow of fuel can be controlled via remotely activated valves and pumping systems, which not only provides a means of securing the fire exposure once a reaction occurs but also allows the operator to prolong the exposure in the event that the reaction does not occur in the estimated time frame.

Another benefit of the alternative fuel fire scenarios is that due to the momentum-driven fuel sprays being produced by both alternative fuel fires, the fires are less susceptible to wind effects than the standard STANAG 4240 pool fire. In the standard pool fire, fuel vapors are transported via thermal buoyancy, diffusion, and air entrainment, all of which are very susceptible to wind effects. Due to the fact that in both alternative fuel fire scenarios the fuel is being emitted from a nozzle(s) at a set pressure, the fuel emitted has upward momentum, which makes the fuel spray less susceptible to wind effects. This benefit can potentially allow the test operator to use smaller exposure area given that the fire plume is less likely to bend in the direction of the prevailing wind and expose the container being tested.

With respect to repeatability, the alternative fuel fire exposures provide increased repeatability in that they utilize the same fuel (i.e., propane or heptane) from test to test. This differs from the approach used in STANAG 4240, which does not require a specific fuel but instead provides a range of fuels that can be used. Currently, all STANAG 4240 approved fuels are multi-constituent hydrocarbons whose blends can vary from manufacturer to manufacturer and season to season. While the effect of variation in fuel blends is not expected to have a significant influence on the thermal exposure to the test article, it is still a variable that must be considered when addressing repeatability from test to test.

6.3 Environmental Impacts

A limited number of locations perform STANAG 4240 pool fire tests in the United States due to the high cost and unique requirements of the test. Such locations include Aberdeen Proving Ground, MD, Naval Surface Warfare Center Dahlgren, VA, Naval Air Warfare Center China Lake, CA, National Technical Systems, AR, and General Dynamics, FL. In general, the same types of release, emission and exposure concerns apply at all locations; however, State, regional and local regulations and permitting requirements impact each test facility differently.

One location that conducts a variety of pool fire tests, including STANAG 4240 pool fire tests and "bonfire" tests, is presented herein for reference and considered typical of other similar locations. The operator conducts pool fires under a special air quality permit issued by its State

Department of Environmental Quality (DEQ) separately from other air emission permits. This additional permit requires that pool fire tests be conducted in accordance with an approved standard operating procedure that was jointly developed by the operator and the State DEQ. The operator is required to document and report annual quantities of fuel consumed in the tests, provide daily notifications of scheduled tests, and submit to quarterly test site inspections by the State DEQ. The standard operating procedure stipulates that burn pits be surrounded with a bed of sand to control accidental fuel spills and assumes that any fuel in the sand will be consumed by the excess heat in the pits. The operator conducts an estimated 150 pool fire burns per year, with the majority of those being STANAG 4240 pool fire tests. Depending on local and regional ambient air quality concerns, other locations may be limited in the number of tests they can conduct per year and in the particular days on which they are permitted to test.

6.3.1 Spill Prevention, Control and Countermeasures

Per the requirements of section 4 of the specification for standard liquid fuel/external fire test described in STANAG 4240, suitable liquid hydrocarbon fuels are JP-4, JP-5, Jet A-1, AVCAT, or commercial grade kerosene. As such, there is a risk of fuel spills on the test site. Oil Spill Prevention, Control and Countermeasures (SPCC) regulations outline requirements for petroleum-based fuels and refined petroleum products (*20*). The Environmental Protection Agency (EPA) does not publish an inclusive list of such products, instead delegating this responsibility to the enforcing agency at the State and local level; however, the Coast Guard does publish a list of products that it considers to be "oil" and therefore potentially subject to SPCC requirements (*21*). All of the fuel blends identified in STANAG 4240 plus heptane are identified on the Coast Guard list, but propane is not. In addition, the EPA specifically excludes propane from SPCC requirements (*20*). Based on these designations, any location conducting STANAG 4240 pool fire tests would be subject to SPCC requirements if its combined aboveground "oil" storage capacity exceeds 1320 gal. All storage, piping, and transportation equipment and facilities related to the pool fire operation would need to be addressed in the facility SPCC plan, which may contain extensive and costly measures for containment, drainage, and cleanup (*20*). The proposed propane-based alternative test methods could offer significant benefits in this area.

In more general terms, the STANAG 4240 fuel blends can be classified as middle distillates containing paraffins, cycloparaffins, aromatics, and olefins, from approximately C_9 to C_{20}. If these fuels were accidentally released or spilled, some short-term hazards may result from the more volatile and water soluble compounds, such as toxicity to aquatic life in the water column as well as potential inhalation hazards (e.g., narcosis). These fuels also pose a moderate to high acute toxicity to biota with product-specific toxicity to aromatic compounds. All of the STANAG 4240 fuel blends are derived from petroleum and are known to contain a variety of potentially toxic materials, most commonly polycyclic aromatic hydrocarbons (PAHs).

Examples include naphthalene, anthracene, and other ring compounds. The health effects of PAHs can vary from material to material, but PAHs can be extremely toxic. Several PAHs are

listed by the EPA as probable human carcinogens. The EPA has designated 32 PAH compounds as priority pollutants under the Clean Water Act and can regulate the materials as such in the case of a spill (*22*). The proposed heptane and propane alternatives pose lower risk of liquid fuel coming into contact with the ground beneath the spray nozzles given that the nozzles were designed to produce an atomized spray of fuel that is generally entrained/consumed in the combusting fire plume. However, in the event that liquid heptane or propane was to reach an unprotected ground surface, the liquid would be expected to biodegrade to a moderate extent. Furthermore, if released into the soil, the liquid would not be expected to leach into groundwater due to its high volatility.

6.3.2 Air Emissions

In addition to the potential environmental hazards associated with these medium distillate fuels being in contact with soil and water, there are also substantial environmental impacts associated with their combustion and the resulting emissions. When burned in open pools, as specified in STANAG 4240, the combustion is generally inefficient resulting in increased production of soot. Soot is often measured and regulated as opacity, which is the amount of light that can pass through a medium. Opacity is reported as a percentage—0% opacity means that all light passes through and 100% opacity means that no light passes through. EPA measures opacity from stationary sources such as smoke stacks by using New Source Performance Standard Test Method 9: Visual Determination of the Opacity of Emissions from Stationary Sources (*23*). There is no national standard for opacity from open burning; however, individual States and localities can and often do apply Method 9 to a variety of emission sources at their discretion.

When combusted in bench-scale test apparatus, fuels such as kerosene have a soot yield of 0.097 ± 0.016 g/g fuel. When combined with the fact that the STANAG 4240 test fires generally cover very large areas, these tests can emit substantial quantities of particulate into the air.

Representative photographs of the smoke plume resulting from (a) a 2.2 m (7.2 ft) square JP-4 pool fire burning at a rate of ~0.41 g/s, (b) a heptane spray fire burning at a rate of 0.17 g/s, and (c) a propane spray fire burning at a rate of nominally 0.04 g/s are provided in figure 53.

As shown in figure 53a, the combustion of the medium distillate fuels specified in STANAG 4240 produce a very large, very sooty smoke plume that extends well into the atmosphere above the fire. Also shown in figure 53 are the smoke plumes emanating from both the heptane and propane spray fires evaluated. These plumes are far less soot-laden, with the heptane spray fire producing some soot and the propane fire producing very little, if any, visible smoke. To further confirm the drastic decrease in smoke production afforded by both alternative fuel fire exposures being considered, a total mass of soot produced by each fire scenario was calculated and is presented in table 19. These soot yields were calculated using an assumed 12 min burning duration, the yield data provided in table 11, and the mass burning rates listed earlier in this section.

STANAG 4240 Pool Fire (b) Heptane Spray Fire (c) Propane Spray Fire

Figure 53. Comparison of photographs.

Table 19. Total soot yields for STANAG 4240 and alternative fuel fire exposures.

Fuel Type	Soot Yield (g/g)	Total Mass of Soot Released (kg [lb])
STANAG 4240 fuels	0.097	16.3 [36]
Heptane	0.015	2.1 [4.6]
Propane	0.004	—

As shown in table 18 and while from a quantity-consumed standpoint, the heptane spray fire exposure provides substantial savings. Due to the increased cost of the fuel, the cost savings are negated. However, this is not the case for the propane exposure fires, which show substantial fuel and fuel cost savings when compared to the standard STANAG 4240 liquid pool fire exposure. Given that the cost of the propane and STANAG 4240 liquid fuels is equivalent, the fuel cost savings associated with the use of propane are comparable to fuel quantity savings (i.e., 58%–84%).

It should be noted that the cost savings just presented are strictly based upon fuel costs and do not take into the account the increased facilities and operational costs associated with the storage, transport, and vaporization of large quantities of propane. While these costs are expected to be significant, it is also expected that the bulk of the expense will be a one-time cost for the installation/commissioning of the facility, and, once commissioned, the operating costs should not be such that the savings provided by the use of the propane is negated.

In addition to the more direct issues associated with opacity, soot generated from combustion sources is under increased scrutiny as it has also been linked to global climate change, particularly in snow-covered areas. When deposited on snow or ice, soot can lower the surface albedo, or the reflecting power of the surface, allowing more heat to be absorbed and increasing ice melt. Although not a regulated concern currently, this issue may be of increased concern in the future due to the focus on global climate change (*24*).

6.3.3 Occupational Exposure

Recommended safe occupational exposure levels are set by the Occupational Safety and Health Administration (OSHA). The applicable OSHA Permissible Exposure Limits (PELs), as well as Recommended Exposure Levels (published by the National Institute for Occupational Safety and Health) and Threshold Limit Values (published by the American Conference of Industrial Hygienists) for the STANAG 4240 fuel blends and the proposed alternatives, are provided in table 20. Although only the OSHA PELs are legally enforceable, government and commercial facilities often adopt the most stringent of the three types of standards. There are no specific exposure standards for the fuel blends; however, the majority of the STANAG 4240 blends contain kerosene, which will be used for this assessment. It should be noted that the exposure

scenarios for pool fire testing are well ventilated outdoor environments, but the values in table 20 are still important for acute, localized exposures. The alternative fuels have much higher (i.e., less stringent) PELs than the current liquid fuels and, as such, should pose less of a risk to the test operators. In addition, the current STANAG 4240 test method involves hands-on, open exposures to bulk fuels while the alternatives are enclosed piping systems that can be controlled remotely, thereby minimizing operator exposure to the fuels.

Table 20. Occupational exposure limits for current and alternative fuels.

		OSHA PEL (*25*)	**NIOSH REL (*26*)**	**ACGIH TLV (*27*)**
Alternatives	**Heptane**	500 ppm 2000 mg/m^3 TWA	85 ppm 350 mg/m^3 TWA	400 ppm 1640 mg/m^3 TWA
	Propane	1000 ppm 1800 mg/m^3 TWA	1000 ppm 1800 mg/m^3 TWA	1000 ppm 1800 mg/m^3 TWA
Current	**JP-4**			
	kerosene	NA	100 mg/m^3 TWA	200 mg/m^3 TWA
	JP-5 (aka JET A-1)			
	kerosene	NA	100 mg/m^3 TWA	200 mg/m^3 TWA
	naphthalene	10 ppm 50 mg/m^3 TWA	10 ppm 50 mg/m^3 TWA	10 ppm 50 mg/m^3 TWA
	JP-8			
	kerosene	NA	100 mg/m^3 TWA	200 mg/m^3 TWA
	naphthalene	10 ppm 50 mg/m^3 TWA	10 ppm 50 mg/m^3 TWA	10 ppm 50 mg/m^3 TWA

As shown in table 18 and while from a quantity consumed standpoint, the heptane spray fire exposure provides substantial savings. Due to the increased cost of the fuel, the cost savings are negated. However, this is not the case for the propane exposure fires, which show substantial fuel and fuel cost savings when compared to the standard STANAG 4240 liquid pool fire exposure. Given that the cost of the propane and STANAG 4240 liquid fuels is equivalent, the fuel cost savings associated with the use of propane are comparable to fuel quantity savings (i.e., 58%–84%).

It should be noted that the cost savings just presented are strictly based upon fuel costs and do not take into the account the increased facilities and operational costs associated with the storage, transport, and vaporization of large quantities of propane. While these costs are expected to be significant, it is also expected that the bulk of the expense will be a one-time cost for the installation/commissioning of the facility and once commissioned the operating costs should not be such that the savings provided by the use of the propane is negated.

6.3.4 Summary of Environmental Impacts

The alternative methods are more environmentally sustainable than the baseline STANAG 4240 test method. Although the current method is operated in compliance with applicable Federal, State and local regulations, it is likely that future regulatory actions against soot, PM and HAPs will continue to become more stringent. The alternative methods produce less soot, do not use HAPs, and pose a lower risk for occupational and environmental exposures, all of which contribute to reduced compliance risk. The heptane spray fire poses very little ground contamination potential and reduces air pollution by a factor of ~8 while the propane fire exposure poses near zero potential for ground contamination or air pollution. In general, the proposed alternative fuel fire exposures are beneficial with respect to cost, control, and environmental impact when compared to the existing STANAG 4240 liquid fuel fire exposure. As the need for this type of testing increases to support the demand for new IM qualified munitions, more sustainable test methods need to be further developed and pursued for implementation.

---

7. Conclusions

Recently, there has been an international push to develop/institute alternative fuel fire exposures to be used in place of the STANAG 4240 fire scenario due to an overall lack of control over the current fire scenario as well as the environmental implications associated with the hydrocarbon pool fire. Based upon this push, a test program was developed. The program consisted of the following:

- Developing a robust, fully-instrumented container to characterize the thermal response of an object to the various fire exposures;
- Characterizing the thermal exposure generated by the STANAG 4240 liquid fuel external fire exposure to serve as a baseline to which all alternative fuel fire exposures are compared; and,
- Developing and testing two different alternative fuel exposure fire scenarios designed to mimic the heating rate and spatial uniformity of the STANAG 4240 exposure while addressing the current environmental issues with the existing test method.

7.1 Development of Instrumented Container

In this work, two identical, instrumented containers simulating the PA-124 container were developed, constructed, calibrated, and commissioned. The boxes were designed to represent the structure of the PA-124 munitions container. The boxes were shown to be able to survive prolonged fire exposures with minimal thermal degradation and provide accurate estimates of

thermal heat flux exposure. The boxes were constructed to measure incident heat flux to the surfaces of the container using plate thermometers. Calibration and commissioning of the boxes/plate thermometers was accomplished using a UL 1709 furnace exposure which provided a simple and repeatable exposure test for applying rapidly increasing heat flux exposure to the box. The methods of Ingason and Wickstrom (*8*) were shown to produce accurate values when calculating the incident radiative heat flux to the plate thermometers and the box surfaces. The measured surface temperatures were used in simple calculations and shown to measure the incident heat fluxes, demonstrating a linear relationship between calculated and actual heat fluxes with average regression coefficients (r) of 0.945 for the box surfaces and 0.991 for the plate thermometers. The plate thermometers were shown to provide the best estimate of radiant heat flux, which will allow for estimates of incident heat fluxes to be made during future exposure testing where installation of heat flux gauges is not possible, such as during large pool fires. Based upon these results, the instrumented containers were considered to be calibrated and could be used to characterize the thermal exposures generated during the liquid fuel/external fire test prescribed in STANAG 4240.

7.2 STANAG 4240 Exposure Characterized

Four STANAG 4240 exposure fires were conducted in a 2.2 m (7.2 ft) square fuel pan filled with 208 L (55 gal) of JP-5 fuel. The fires burned for an average of 12 min, with 2.9–5.8 kph (1.8–3.6 mph) average wind speeds during testing. Average flame temperatures measured in close proximity to the container ranged from 697 to 763 °C (1286 to 1406 °F), with maximum flame temperatures as high as 978 °C (1792 °F). These thermal exposure data, while being on the low end, are generally consistent with available data for large-scale pool fires which can range from 770–1200 °C (1418–2192 °F) (*12*). Under these conditions, the aforementioned instrumented box measured average incident heat fluxes ranging from 36 to 103 kW/m^2 over the test duration, depending upon where the measurement was taken. Maximum measured heat flux values were as high as 150 kW/m^2. The average incident heat fluxes measured during these tests were generally lower than those reported in the literature for objects immersed in a pool fire. However, several studies (*9, 12*) report lower incident heat flux measurements for objects immersed in pool fires where the object size is comparable to that of the pool fire. In these studies (*13, 14*), maximum average heat flux measurements of 75–85 kW/m^2 were reported and attributed to the object reducing the local flame temperatures, thus reducing the thermal insult.

In the tests conducted, the container remained immersed in the flame plume the majority of the time the liquid fuel fires were burning. However, at times of extreme wind conditions, the container was exposed to ambient conditions for periods of time ranging in duration from seconds to tens of seconds. This wind effect coupled with the inherent temperature differences within the fire plume, even under quiescent conditions, and resulted in some thermal exposure differences with respect to the orientation of the container. In general, the vertical sides of the container (i.e., sides of the container that were perpendicular to the fuel surface) were subjected

to the most severe thermal exposures, with the horizontal surfaces being exposed to slightly less severe conditions. On average, the exposures to the vertical surfaces were 10–36 kW/m^2 greater than those measured on the horizontal surfaces. The data collected in this task characterized the thermal exposure to a container from a STANAG 4240 fire exposure and were used as baseline data to which the thermal exposures generated by alternative fuel fire exposures were compared.

7.3 Characterization of Alternative Fuel Fire Exposures

Four alternative fuel fire exposures were conducted using the same experimental test setup used in the aforementioned STANAG 4240 liquid fuel fire exposures. The alternative fuel fire exposures considered were a heptane spray fire, a propane area burner, and pair of propane line burners. Heptane and propane were selected as alternative fuels because they represent both a liquid and gaseous fuel with similar heats of combustion, only more volatile and less sooty than STANAG 4240 allowed fuels when combusted. The fires were generally permitted to burn for 11–14 min, with 1.8–3.6 kph (1.1–3.2 mph) average wind speeds. Average flame temperatures for these tests ranged from 673 to 929 °C (1244 to 1705 °F), with maximum flame temperatures as high as 1099 °C (2010 °F). Under these conditions, the instrumented box measured average incident heat fluxes ranging from 33 to 109 kW/m^2 over the test duration, with maximum measured heat flux values as high as 175 kW/m^2. In general, the temperature and heat flux data collected in these alternative fuel fire exposures were comparable to that measured in the STANAG 4240 pool fires with the heptane spray fires being consistently hotter and the propane fires being consistently lower.

Given that the alternative fuel fire exposures produced generally similar thermal exposures, they were also evaluated with respect to the additional benefits these exposures had over the existing liquid fuel fire exposure. The benefits considered in this work were in relation to the cost of operation, added control over exposure, and environmental impact. When evaluated for the cost of operation, it was determined that although less fuel is consumed with the proposed heptane spray fire. Due to the cost of heptane being almost double that of the currently specified STANAG 4240 fuels, the fuel for the heptane spray burner would cost more. When considering propane, the upfront costs associated with test facility setup to accommodate the new fuel would be significant, but, once accounted for, implementation of the propane fuel provides substantial fuel cost savings. When control over the exposure fire was considered, it was evident that either alternative fuel fire exposure provided an increased level of control to the test operator. Finally, with respect to environmental impact, it was shown that the heptane spray fire produces a smoke plume that is approximately one-eighth that of the STANAG 4240 exposure, while the propane produces a negligible amount of smoke (i.e., barely visible).

8. Future Work

Although both alternative fuel fire exposures developed in this work produced thermal exposures that were comparable to that of the STANAG 4240 liquid fuel fire, there are numerous improvements and potential issues with these fires that should be addressed prior to full-scale validation testing being performed. Improvements to the alternative fuel fire exposures could include optimization of the nozzles used and/or the configuration in which the nozzles are installed. In both cases, this optimization could result in a more uniform thermal exposure that is potentially less susceptible to wind effects than the current approach, which delivers all fuel from beneath the test article. Optimization of the nozzle spray could also increase combustion efficiency, which could result in a further reduction in smoke production and an enhancement of the severity of the thermal exposure to the test article. In addition to the optimization of the alternative fuel fire exposures, potential issues associated with these scenarios should also be investigated. In previous studies (*28*) evaluating the use of propane as a fuel for thermal shock testing, it was determined that "hot spots" can develop when a fuel is being sprayed proximate to an object. The prevalence/absence of these localized areas of elevated temperatures (i.e., hot spots) in the proposed alternative fuel fire exposures should also be investigated to ensure that artificial test results are not obtained.

9. References

1. TB700.2. Department of Defense Ammunition and Explosives Hazard Classification Procedures, U.S. Department of Defense, NAVSEAINST 8020.8B, 1998.
2. MIL-STD-2105C. *Hazard Assessment Tests for Non-Nuclear Munitions* **2003**.
3. STANAG 4240. *Liquid Fuel/External Fire, Munition Test Procedures*, North Atlantic Treaty Organization (NATO), **2003**.
4. STANAG 4439. *Policy for Introduction, Assessment and Testing for Insensitive Munitions (MURAT)*, North Atlantic Treaty Organization (NATO), **2003**.
5. Tanner, S. Propane as a Surrogate for Kerosene in Fuel Fire Tests. Presentation given at the Department of Defense Explosive Safety Board (DDESB) Meeting, 2010.
6. Underwriters Laboratories, Inc. *Rapid Rise Fire Tests of Protection Materials for Structural Steel*; UL 1709; Northbrook, IL, 1998.
7. ISO 834. *Fire-Resistance Tests - Elements of Building Construction -- Part 8: Specific Requirements for Non-Load Bearing Vertical Separating Elements*, International Standards Organization, 2002.
8. BS/EN 1363-1. *Fire Resistance Tests - Part 1 General Requirements*, British Standards, 1999.
9. Ingason, H.; Wickstrom, U. *Measuring Incident Radiant Heat Flux Using the Plate Thermometer*, SP Swedish National Testing and Research Institute, Department of Chemistry and Fire Technology, 2006.
10. Churchill, S. W.; Chu, H. H. S. Correlating Equations for Laminar and Turbulent Free Convection from a Vertical Plate. *Int. J. Heat Mass Transfer* **1975**, *18*, 1323.
11. Childs, K. W. *HEATING 7: Multidimensional, Finite-Difference Heat Conduction Analysis Code System*; technical report PSR-199; Oak Ridge National Laboratory (ORNL): Oak Ridge, TN, 1998.
12. Heat Release Rates. *Society of Fire Protection Engineers Handbook of Fire Protection Engineering*; 3rd ed.; Society of Fire Protection Engineering: Bethesda, MD, 2008.
13. McLain, W. H. *Investigation of the Fire Safety Characteristics of Portable Tanks Polyethylene Tanks Containing Flammable Liquids*; report no. CG-M-1-88; U.S. Coast Guard: Washington, DC, 1998.

14. Taylor, A. J. et al. *Engulfment Fire Tests on Road Tanker Sections*; Rarde technical report 7/75; Controller HMSO, London, 1975.

15. Fire Hazard Calculations for Large, Open, Hydrocarbon Fires. *Society of Fire Protection Engineers Handbook of Fire Protection Engineering*; 3rd ed.; Society of Fire Protection Engineering: Bethesda, MD, 2008.

16. Hamins, A.; Maranghides, A.; Mulholland, G. *The Global Combustion Behavior of 1MW to 3MW Hydrocarbon Spray Fires Burning in an Open Environment*; NISTIR 7013; National Institute of Standards and Technology: Gaithersburg, MD, 2003.

17. Gottuk, D.; Mealy, C.; Floyd, J. Smoke Transport and FDS Validation, Fire Safety Science. *Proceedings of the 9th International Symposium*, International Association of Fire Safety Science, Karlsruhe, Germany, 21–26 September, 2008; pp 129–140.

18. ASTM STP 1284. Fire Resistance of Industrial Fluids. *Annu. Book ASTM Stand*. **1996**.

19. Barrington, L. M. *Full-Scale Insensitive Munitions Testing of the RAN 5"/54 Cartridge Case*; DSTO-TR-0097; Explosives Ordnance Division, Aeronautical and Maritime Research Laboratory: Australia, 1997.

20. Applicability, Definitions, and General Requirements for All Facilities and All Types of Oils. Code of Federal Regulations Title 40, Pt. 112, 2009.

21. U.S. Department of Homeland Security. List of Petroleum and Non-petroleum Oils. U.S. Coast Guard. http://www.uscg.mil/vrp/faq/oil.shtml (accessed 16 June 2008).

22. 126 Priority Pollutants. Code of Federal Regulations, Title 40, Appendix A to pt. 423.

23. Compliance With Standards and Maintenance Requirements. Code of Federal Regulations, Title 40, pt. 60.11(b), 2000.

24. Integrated Assessment of Black Carbon and Tropospheric Ozone, UNEP and WMO, 2011.

25. Limits for Air Contaminants. Code of Federal Regulations, Title 29, pt. 1910.1000 Table Z-1, 2006.

26. U.S. Department of Health and Human Services. NIOSH Pocket Guide to Chemical Hazards. Centers for Disease Control and Prevention: Washington, DC, September 2007.

27. Documentation of the TLVs and BEIs, ACGIH, 2009.

28. Ford, K. P.; Davis, N. C.; Farmer, A. D.; Washburn, E. B.; Atwood, A. I.; Wilson, K. J.; Abshire, J. P.; Shewmaker, M. L.; Goedert, Z. P.; Wheeler, C. J. *Subscale Fast Cook-off Test Results*, Insensitive Munitions European Manufacturers Group, 2010.

NO. OF COPIES	ORGANIZATION
1 (PDF only)	DEFENSE TECHNICAL INFORMATION CTR DTIC OCA 8725 JOHN J KINGMAN RD STE 0944 FORT BELVOIR VA 22060-6218
1	DIRECTOR US ARMY RESEARCH LAB IMNE ALC HRR 2800 POWDER MILL RD ADELPHI MD 20783-1197
1	DIRECTOR US ARMY RESEARCH LAB RDRL CIO LL 2800 POWDER MILL RD ADELPHI MD 20783-1197

NO. OF COPIES ORGANIZATION

1 DIR US ARMY RSRCH LAB
RDRL SE
T BOWER
2800 POWDER MILL RD
ADELPHI MD 20783-1197

1 DIR US ARMY RSRCH LAB
RDRL CI
J PELLEGRINO
2800 POWDER MILL RD
ADELPHI MD 20783-1197

1 DIR US ARMY RSRCH LAB
RDRL SES P
M SCANLON
2800 POWDER MILL RD
ADELPHI MD 20783-1197

2 US ARMY RSERCH OFC
D STEPP
S MATHAUDHU
PO BOX 12211
RESEARCH TRIANGLE PARK NC
27709-2211

3 DARPA
DEFNS SCI OFC
M MAHER
J GOLDWASSER
S WAX
3701 N FAIRFAX DR
ARLINGTON VA 22203-1714

1 DIR DFNS INTLGNC AGCY
TA 5
K CRELLING
WASHINGTON DC 20310

12 HUGHES ASSOC INC
J FLOYD (2 CPS)
C MEALY (2 CPS)
P TAYLOR (2 CPS)
J DINABURG (2 CPS)
D VERDONIK 2 (CPS)
N LIEB (2 CPS)
3610 COMMERCE DR
STE 817
BALTIMORE MD 21227-1652

NO. OF COPIES ORGANIZATION

ABERDEEN PROVING GROUND

27 DIR USARL
RDRL VTM
V WEISS
RDRL WM
L BURTON
B FORCH
S KARNA
J MCCAULEY
P PLOSTINS
W WINNER
RDRL WML
T VONG
M ZOLTOSKI
RDRL WML D
A HORST
RDRL WML E
R ANDERSON
RDRL WML F
D LYON
RDRL WMM
J BEATTY
R DOWDING
P SMITH (3 CPS)
J ZABINSKI
RDRL WMM D
E CHIN
R SQUILLACIOTI
RDRL WMP
P BAKER
W RUPPERT (3 CPS)
S SCHOENFELD
RDRL WMS
T ROSENBERGER
S TAULBEE

INTENTIONALLY LEFT BLANK.